Universidad de Valladolid

DOCTORAL PROGRAMME IN PHYSICS

DOCTORAL THESIS:

Quantum vacuum energy in cavities: from singular interactions to magnetodielectrics

Thesis submitted by:

César Romaniega Sancho

as part of the requirements for the degree of DOCTOR *by the University of Valladolid*

Supervised by:

Luis Miguel Nieto Calzada
José María Muñoz Castañeda
Inés Cavero Peláez

Universidad de Valladolid

PROGRAMA DE DOCTORADO EN FÍSICA

TESIS DOCTORAL:

Energía de vacío cuántica en cavidades: de interacciones singulares a magnetodieléctricos

Presentada por:

César Romaniega Sancho

para optar al grado de Doctor por la Universidad de Valladolid

Dirigida por:
Luis Miguel Nieto Calzada
José María Muñoz Castañeda
Inés Cavero Peláez

To my family

"If you are receptive and humble, mathematics will lead you by the hand."

Paul Dirac

Acknowledgements

La presentación de esta tesis doctoral culmina una etapa que ha estado acompañada de innumerables lecciones y gracias a las personas adecuadas ha dado lugar a una experiencia realmente valiosa.

En primer lugar, me gustaría agradecer a mis tutores por su dedicación durante este periodo. A Luis Miguel Nieto como director por hacer que esta tesis pudiera salir adelante desde el primer momento, teniendo la puerta siempre abierta para hacerme la vida más sencilla. También a José María Muñoz e Inés Cavero, en especial por facilitar mi adaptación al mundo académico. De una forma u otra, todo lo que he aprendido durante estos años ha surgido de estas relaciones.

No menos importante, quiero agradecer a mi familia y amigos. A mis padres por todo el esfuerzo dedicado para que hoy pueda estar culminando mi tesis doctoral. Gracias por hacer que nunca me haya faltado nada y por inculcarme esos valores que me han hecho llegar hasta aquí. También a mis hermanos, Álvaro y Sara, un apoyo constante durante estos años fruto de nuestra particular sinergia.

I also want to thank Guglielmo Fucci for his kind hospitality in North Carolina. I really appreciate all the time and effort you invested for making the most of my research stay at East Carolina University. Thank you for all the bountiful knowledge, from spectral zeta functions to sailing lessons on the Neuse River.

Por último, a mis compañeros de Departamento, en particular a Lucía y Marcos, con quienes más momentos he tenido la suerte de compartir. También a todos los profesores de los que he ido aprendiendo a lo largo de estos años en Valladolid. En especial a Manuel Gadella por su innegable vocación. Esta ha influido directamente en mi formación desde que fuera su alumno durante la carrera hasta ahora, con uno de nuestros artículos formando parte de esta tesis.

A todos vosotros, gracias.

Esta tesis ha sido financiada a través de un contrato de Formación de Profesorado Universitario (FPU17/01475), que fue concedido por el Ministerio de Educación, Cultura y Deporte. La estancia de investigación en el Departamento de Matemáticas de East Carolina University (North Carolina, USA) fue financiada a través del programa de Ayudas complementarias de movilidad (EST21/00286) del Ministerio de Universidades.

Abstract

This thesis presents an analysis of the Casimir-Lifshitz effect for configurations of two objects, being one of them contained within the other. The first of the two parts of this work is devoted to the construction and study of a particular family of potentials that will be used for mimicking the bodies. The aim is to employ a potential simple enough for obtaining some nontrivial analytical results. This will help us to gain some insight in the properties of the quantum vacuum for these systems and thus be able to present general results for more realistic systems. To that end, we use a generalization of the Dirac δ, the so-called δ-δ' interaction, extending the one-dimensional definition to spherical systems for spatial dimension $d \geq 2$. The definition is based on constructing self-adjoint extensions of the original Hamiltonian. We perform a study of the domain and spectrum of the resulting operator, indicating some possible applications in quantum mechanics, in particular within the context of mean-field nuclear models. For this reason, we add nonsingular potentials to the δ-δ' interaction such as the spherical well and a Coulombic term, suitable to describe neutron and proton energy levels. We show that general features of the low-energy states can be obtained, indicating how these singular interactions can be used as a first approximation for real physical systems in certain contexts.

The second part of the thesis is devoted to the proper study of the vacuum energy in cavity configurations. The main goal is to expand the analysis of the Casimir effect to this kind of configurations, establishing some general results on the sign of the energy and pressure. Thus, we first study a massless scalar field in the presence of two concentric δ-δ' spheres. For computing the pressure on the spheres, the interaction energy between them and the self-energy should be considered. On this basis, we first study the interaction between the spheres employing the TGTG representation. The interaction energy is known to be free of divergences. However, this is not the case for the self-energy. In order to regularize this quantity we employ the zeta function regularization method. Studying the structure of the divergences we find a one-parameter family of potentials in which the self-energy and self-pressure are unambiguously defined. The latter is based on the cancellation of the heat kernel coefficient a_2, so no renormalization procedure is needed. Bearing in mind the results obtained for the interaction energy for the scalar field, some general results for the electromagnetic field are obtained also employing the TGTG representation. In particular, we consider two different configurations: a dielectric sphere enclosed within an arbitrarily shaped magnetodielectric cavity and a dielectric object with a spherical cavity in which another arbitrarily shaped magnetodielectric object is enclosed. For the latter, some new results in classical scattering theory for experiments in which source and detector are inside an object are presented. As for the scalar field, the self-energy is also considered when computing the total pressure. In this case, for one of the few configurations in which the self-energy is unambiguously defined for material bodies, a dilute dielectric ball.

Resumen

Esta tesis presenta un estudio del efecto Casimir-Lifshitz para configuraciones de dos objetos, estando uno de ellos contenido dentro del otro. La primera de las dos partes de este trabajo está dedicada a la construcción y estudio de una familia de potenciales singulares que se utilizarán para modelar los cuerpos. El objetivo es emplear un potencial suficientemente simple pero que dé lugar a resultados analíticos no triviales. Esto facilitará la comprensión de las propiedades del vacío cuántico para estos sistemas para así ser capaces de presentar resultados generales para sistemas más realistas. Para ello, utilizamos una generalización de la δ de Dirac, la llamada interacción δ-δ', extendiendo la definición unidimensional a sistemas esféricos de dimensión espacial $d \geq 2$. La definición se basa en la construcción de extensiones autoadjuntas del hamiltoniano original. Realizamos un estudio del dominio y espectro del operador resultante, indicando algunas posibles aplicaciones en mecánica cuántica, en particular para modelos nucleares de campo medio. Por esta razón, añadimos potenciales no singulares a la interacción δ-δ' como el pozo esférico y un término coulombiano, adecuados para describir los niveles de energía de neutrones y protones. Mostramos que se pueden obtener características generales de los estados de baja energía, indicando cómo estas interacciones singulares sirven como primera aproximación para sistemas físicos en ciertos contextos.

La segunda parte de la tesis está dedicada al estudio de la energía del vacío en configuraciones con una cavidad. El objetivo principal es ampliar el análisis del efecto Casimir-Lifshitz a este tipo de sistemas, demostrando resultados generales sobre el signo de la energía y la presión. De esta forma, primero estudiamos un campo escalar sin masa en presencia de dos esferas δ-δ' concéntricas. Para calcular la presión sobre las esferas debemos considerar la energía de interacción entre ellas y también la autoenergía de cada una por separado. De esta forma, primero estudiamos la interacción entre las esferas empleando la representación TGTG de la energía, la cual da lugar a una energía y fuerza finita. Sin embargo, lo mismo no ocurre para la autoenergía. Para regularizar esta cantidad empleamos el método basado en funciones zeta. Estudiando la estructura de las divergencias encontramos una familia uniparamétrica de potenciales en la que la autoenergía y la presión están definidas de forma inequívoca. Esto último se basa en la cancelación del coeficiente del núcleo de calor a_2, por lo que no se necesita ningún procedimiento adicional de renormalización. Teniendo en cuenta los resultados obtenidos para la energía de interacción con el campo escalar, hemos demostrado resultados generales para el campo electromagnético, usando también la representación TGTG. En particular, hemos considerado dos configuraciones diferentes: una esfera dieléctrica encerrada dentro de una cavidad magnetodieléctrica con geometría arbitraria y un objeto dieléctrico con una cavidad esférica en la que está encerrado otro objeto magnetodieléctrico también con geometría arbitraria. Para probar esto hemos introducido nuevos resultados en el contexto de la teoría clásica de scattering para experimentos en los que la fuente y el detector están dentro del objeto. Al igual que para el campo escalar, la autoenergía también se ha considerado al calcular la presión total. En este caso, para uno de los pocos sistemas en los que la autoenergía se define sin ambigüedades para objetos materiales, una esfera dieléctrica en el límite diluido.

Contents

List of Figures

Publications

The work presented in this thesis has given rise to the following publications:

1. J. M. Muñoz-Castañeda, L. M. Nieto and C. Romaniega, *Hyperspherical δ-δ' potentials*, Ann. Phys. **400**, 246 (2019).

2. C. Romaniega, M. Gadella, R. M. Id Betan and L. M. Nieto, *An approximation to the Woods–Saxon potential based on a contact interaction*, Eur. Phys. J. Plus **135**, 372 (2020).

3. L. M. Nieto, M. Gadella, J. Mateos-Guilarte, J. M. Muñoz-Castañeda, and C. Romaniega, "Some Recent Results on Contact or Point Supported Potentials", in Geometric Methods in Physics XXXVIII. Trends in Mathematics (Springer, 2020), pp.197-219.

4. I. Cavero-Peláez, J. M. Muñoz-Castañeda, and C. Romaniega, *Casimir energy for concentric δ-δ' spheres*, Phys. Rev. D **103**, 045005 (2021).

5. C. Romaniega, *Repulsive Casimir–Lifshitz pressure in closed cavities*, Eur. Phys. J. Plus **136**, 327 (2021).

6. C. Romaniega, *Casimir-Lifshitz pressure on cavity walls*, Eur. Phys. J. Plus **136**, 1051 (2021).

7. A. Martín-Mozo, L. M. Nieto and C. Romaniega, *A solvable contact potential based on a nuclear model*, Eur. Phys. J. Plus **137**, 33 (2022).

8. Casimir self-energy of a δ-δ' sphere, C. Romaniega, I. Cavero-Peláez, and J. M. Muñoz-Castañeda **(pending of acceptance)**.

Introduction

"Summer or autumn 1947, I mentioned my results to Niels Bohr during a walk. That is nice, he said, that is something new... and he mumbled something about zero-point energy. That was all, but it put me on a new track."

H.B.G. Casimir, 1992 [1]

The Casimir effect is a macroscopic manifestation of quantum vacuum fluctuations. It was named after the physicist H. B. G. Casimir, who predicted this phenomenon in 1948 [2]. He was the first to prove that the electromagnetic zero-point energy implies an attractive force between two neutral, parallel, conducting plates at zero temperature. This force between uncharged plates could not be explained by classical electrodynamics, leading to a purely quantum effect arising solely from the modification of the vacuum by the introduction of boundaries. He provided a regularization procedure for dealing with the infinite quantities present in this simple configuration, subtracting the infinite vacuum energy of free Minkowski space from the infinite vacuum energy of the electromagnetic field in the presence of the plates. After removing the regularization, the resulting energy and pressure found were

$$E_0(a) = -\frac{\pi^2\hbar c}{720a^3}, \qquad p_0(a) = -\frac{\mathrm{d}E_0(a)}{\mathrm{d}a} = -\frac{\pi^2\hbar c}{240a^4}.$$

The final expression does not depend on any parameter describing the properties of the plates but only on the distance a between them. This is due to the ideal-metal approximation used for the materials, assuming perfect reflectivity at all frequencies. It is worth noting that the pressure does not depend either on the fine structure constant α of quantum electrodynamics. This results from considering a fluctuating field in a classical background, which is governed by the one-loop effective energy [3]. In consequence, radiative corrections accounting the interaction between photons and electrons are neglected. This is justified for the typical experimental distance 1μm, where these corrections are several orders of magnitude smaller [4] and therefore imperceptible in current measurements. Based on the theory of electromagnetic fluctuations in thermal equilibrium, E.M. Lifshitz a few years later considered the case of two dielectric half spaces separated by vacuum at finite temperatures [5]. Within this approach, Casimir and Casimir-Polder results [2, 6] were obtained as limiting cases. Instead of perfectly conducting metals, the material properties of the bodies were represented by frequency-dependent dielectric response functions, finding that the force[1] between both bodies was also attractive.

After these pioneer works, the interest in the attractive or repulsive character of the force grew over the decades. Historically, the first reason followed from Casimir's semiclassical model for the electron [7]. He suggested that the electron can be modeled by a conductive spherical shell with the electron charge uniformly distributed.

[1] As is customary, we shall refer to this quantity as Casimir or Casimir-Lifshitz force, being the latter more suitable for systems modeled by magnetodielectric response functions.

The repulsive pressure coming from the electrostatic energy, tending to expand the sphere, would be balanced by an attractive force due to vacuum fluctuations, similar to the setup with two plates. Indeed, since the equilibrium condition was independent of the radius, the fine structure constant could be estimated. Unfortunately, Boyer in 1968 proved, after an arduous numerical analysis, that the pressure due to vacuum fluctuations for a conducting sphere also tends to expand the sphere [8]. This result was later confirmed by other authors employing different formalisms [9], like the multiple reflection expansion [10, 11] or the Green's function technique [12]. Based on the latter, it was also found that the force is, however, attractive for a perfectly conducting cylindrical shell [13]. These results led to explore how geometry can affect the character and magnitude of the force. In addition, since 1961 it was known that repulsive forces can also be obtained without assuming idealized metallic surfaces. Dzyaloshinskii, Lifshitz and Pitaevskii (DLP) extended the study of two infinite half-spaces separated by a vacuum gap [5] introducing three different permittivities [14]. They considered two slabs of different materials, labeled 1 and 2, with an intermediate medium, labeled M. The interaction force was expressed as a sum over a set of frequencies with terms proportional to

$$-\left[\varepsilon_1(\omega)-\varepsilon_M(\omega)\right]\left[\varepsilon_2(\omega)-\varepsilon_M(\omega)\right], \tag{1}$$

being ε_i the corresponding permittivities. In 2009, Munday, Capasso and Parsegian were the first to experimentally obtain a repulsive force between material bodies by suitably choosing the permittivities of a sphere, a plate and the intermediate medium ($\varepsilon_1 > \varepsilon_M > \varepsilon_2$) according to DLP's idea [15].

Nowadays, it is known that the force strongly depends on geometry and boundary conditions and this nontrivial dependence is one of the exotic features of this phenomenon [16–18]. However, a satisfactory understanding of this behaviour has not yet been found. The more far-reaching theoretical results have been proved using the representation of the interaction energy in terms of transition matrices [19, 20]. This is often referred to as the representation of the Casimir energy in terms of functional determinants or TGTG representation. For instance, Kenneth and Klich proved that for any mirror symmetric arrangement of objects the force is always attractive [21, 22]. First, note that this is consistent with DLP's result since $\varepsilon_1 = \varepsilon_2$ makes the product (1) negative. More generally, the interaction always leads to attraction between a single object and a plane when both share boundary conditions [3]. Another particular consequence is that although for a conducting sphere an outward pressure arises [8], two conducting hemispheres attract each other at arbitrary short distances. Within this scattering approach, an extension of Earnshaw's theorem can also be proved [23]. This result sets restrictive constraints on the stability of arbitrarily shaped neutral objects held in equilibrium only by Casimir-Lifshitz forces. In particular, the condition for stable equilibrium with dielectric objects is determined by the sign of the expression found by DLP in terms of the product of relative permittivities (1), leading to unstable equilibrium for dielectrics in vacuum.

Aside from the theorems mentioned above, in general, if we want to know the character of the force or the stability of a particular configuration, we are only left with choosing a suitable system of coordinates such that the calculation is feasible[2]. That is to say, whether the interaction force between two arbitrary bodies is attractive or repulsive is in general not known until the explicit calculation is performed. However, a deeper understanding of this phenomenon is relevant for applications,

[2]It is worth mentioning the improvements based on a variable phase method for computing the transition matrices in the TGTG representation for asymmetric bodies [24].

for instance, when designing nanoscale devices with ultra-low stiction [15, 25–27], where the stability of the configuration also plays an important role, especially for levitating devices [15, 26]. Unfortunately, attractive forces are more likely than repulsive ones in current configurations, leading to the stiction problem, the malfunction of microdevices or nanodevices due to the adhesion of some of their components. Some underlying reasons are the Kenneth and Klich theorem [21] and its aforementioned consequences. In addition, the fact that ordinary materials have permittivities higher than vacuum (or air) and permeabilities very close to μ_0 leads to an attractive force according to [14]. In fact, real experiments for material bodies are mostly restricted to planar geometries, generally a sphere and a plate at very short distances. This is the configuration in which the most precise force measurements have been performed, as shown in Ref. [28], where a general review of the experimental work until 2009 can be found. Recent experiments in this context consider predominantly planar geometries as well. For instance, when demonstrating how Casimir-Lifshitz forces can prevent stiction and provide a stable equilibrium for a nanoplate [29] and when these forces are used for self-assembling optical microcavities and polaritons, assuming parallel nanoflakes at short distances [30]. Nonetheless, some methods for avoiding undesired attractive forces in these devices have been proposed. Some of them are explained in detail in the introduction of Chapter 6. For example, instead of parallel plates, *nontrivial* geometries with metallic objects give rise to repulsive forces [31, 32]. However, the equilibrium in these cases is only along the axis of symmetry, making the experimental realization rather challenging. Another proposals are based on the introduction of a chiral medium for avoiding the no-go theorem of Kenneth and Klich [21] and for controlling the strength of the resulting forces in response to an external magnetic field [33]. There is also a novel technique which relies on coating one of the materials with a thin layer of a low-refractive index dielectric in order to obtain a repulsive force at short distances but attractive at long distances, thus realizing stable equilibrium [29]. Indeed, it has been experimentally demonstrated that there is no need to obtain a repulsive Casimir force for avoiding stiction if the system is immersed in a critical binary liquid mixture [34]. In this case the attractive force is counteracted by a repulsive critical Casimir force. The latter can be tailored varying the temperature of the mixture, allowing dynamic control of the nanomechanical system. The critical Casimir forces can be seen as a classical analogue of the Casimir forces due to the fluctuations of the concentrations in the liquid between the surfaces [35].

The above-mentioned work on the Casimir effect has focused primarily on configurations in which the bodies lie outside each other, although some closed cavities have also been considered [36–46]. For instance, a typical system could be a sphere inside the cavity of another object, where the pressure induced on the surface of the sphere by the quantum fluctuations can also be computed. For the study of this quantity, we do not get the full picture if we only consider the interaction energy between both objects. In particular, after subtracting the contribution from free space, the Casimir energy can be written as

$$E_{\mathrm{C}} = E_1 + E_2 + E_{\mathrm{int}},$$

being E_1 and E_2 the self-energies of each object. In the usual case, the force is defined by variations of the distance between bodies, being the self-energies of each body independent of it. This force can be studied between bodies outside each other, as already described, or even when one is inside the other [20, 45]. However, the pressure is defined by variations with respect to the radius of the sphere and its energy E_1 also

depends on it. Since the divergent contributions in the energy depend on the characteristics of each body, the interaction force is always free of divergences [3]. However, a renormalization procedure is in general needed for giving a valid result for the self-energy. Note also that this pressure is the meaningful quantity for configurations like the two concentric shells studied in Chapter 4, where the net force acting on the shells is zero due to the symmetry of the system. It is also worth mentioning that the measurement of this pressure is rather challenging and, to our knowledge, there has not been any experimental attempt yet. However, despite considering cavity configurations, we show that our findings can be checked against experimentally verified results [15], being DLP's setup a limiting case of the system studied in Chapters 6 and 7.

Objectives

As explained, a complete understanding of some essential features of the Casimir-Lifshitz effect has still not been reached. This has encouraged us to pursue in this thesis the objectives summarized below. These will be explained in more detail, together with the main results, in the following section.

- We propose to employ a simple model in order to study the vacuum fluctuations in cavity configurations. The idea is to build a potential for modeling real physical systems in particular contexts. We use a generalization of the Dirac δ, which enables us to obtain nontrivial analytic results. Based on the theory of self-adjoint extensions, we extend previous results for one-dimensional or planar systems. We perform a comprehensive study of the quantum mechanical potential: bound state structure, scattering states and resonances. We show how these singular interactions can be used in physical systems, comparing with the numerical results of well known models such as the phenomenological Woods-Saxon potential.

- We show how the previous analysis within nonrelativistic quantum mechanics (QM) can be used in quantum field theory (QFT) for scalar fields. We first consider a cavity configuration composed of two concentric δ-δ' spherical shells. We propose to understand some features of the interaction energy and self-energy in this context, where the scattering data of the quantum mechanical system will be crucial for computing the interaction energy between the two spherical δ-δ' shells and the self-energy of each one.

- After studying these simple models, we propose to consider more realistic systems. In particular, we study the electromagnetic field coupled to matter described by continuous permittivity and permeability functions, instead of singular interactions. We base our derivation on the TGTG representation and some results of classical electromagnetic scattering. We prove some general features regarding the attractive or repulsive character of the interaction pressure. We are able to determine its sign, under general circumstances, without performing the explicit numerical calculation. We have also developed some new results of classical electromagnetic scattering for the unusual scattering setup needed when studying the interaction energy between one object inside the other.

Main results

In this section we elaborate on the established objectives and the main results of this thesis. We outline the principal features of these findings, showing the purpose of

each objective in connection with the others and reviewing the appropriate literature for each particular topic.

A simple yet complex enough model

The main goal of Part I is to construct and study a model simple enough so it can be solved analytically but with the appropriate number of free parameters to provide insight into some of the features of certain physical systems. Perhaps one of the simplest way to model a body in this context is the use of boundary conditions. For instance, in the original Casimir setup Dirichlet boundary conditions are imposed on the vector potential [3]. As mentioned before, this is clearly an idealization of a real physical body since this model assumes electrons rushing about to counteract any incoming field and the effect of imperfect reflection is known to be large in experiments [16]. The next step could be the introduction of the Dirac delta, which is indeed a generalization of Dirichlet boundary conditions in the so-called strong limit [47]. Contrary to boundary conditions, this potential connects the regions at each side of the boundary. This is why it is often called semitransparent or penetrable boundary condition [48, 49]. In spite of its simplicity, it has a vast amount of applications in modeling real physical systems. A complete set of references can be found in the introductions of Chapters 1, 2, 3 and the references quoted therein. The key point is that this potential enables to obtain a relatively simple solution while keeping the essential properties of the problem. Furthermore, it serves as a fair approximation when the particle wavelength is much larger than the range of the potential, for a very short range interaction between a single particle and a fixed heavy source or for a contact interaction in the center of mass of two particles [50]. In addition, Dirac lattices has also been employed for modeling polarizable sheets [51, 52]

In view of the above, we are going to use a generalization of the Dirac δ potential, the so-called δ-δ' interaction defined in Chapter 1. It was first introduced by Kurasov in Ref. [53], where its definition was based on the theory of self-adjoint extensions. In particular, in one-dimensional QM the corresponding operator can be written as

$$H_1 := -\frac{\mathrm{d}^2}{\mathrm{d}x^2} + a\delta(x) + b\delta'(x), \qquad a, b \in \mathbb{R}, \tag{2}$$

where $\delta(x)$ and $\delta'(x)$ denote the Dirac delta and its *generalized derivative* [53], respectively. In this reference it was proved that this interaction imposes the following matching conditions on the wave function and its derivative

$$\begin{pmatrix} \psi(0^+) \\ \psi'(0^+) \end{pmatrix} = \begin{pmatrix} \frac{2+b}{2-b} & 0 \\ \frac{4a}{4-b^2} & \frac{2-b}{2+b} \end{pmatrix} \begin{pmatrix} \psi(0^-) \\ \psi'(0^-) \end{pmatrix}. \tag{3}$$

If $b = 0$, we have a continuous wave function with a finite jump proportional to the delta coupling for its derivative $\psi'(0^+) - \psi'(0^-) = a\psi(0)$, as expected. Although the definition of the delta is unambiguous, it is also worth mentioning another kind of δ' interaction[3], called nonlocal in Chapters 2 and 3, where this controversy is mentioned.

[3] In some texts, for instance [54], the singular interaction defined by Eq. (3) with $a = 0$ is denoted by $\delta'(x)$, while δ' interaction is used for the definition given by Eq. (4). We will not follow this notation, using δ' interaction for Kurasov's definition along this thesis.

The latter is defined by the matching conditions [55, 56]

$$\begin{pmatrix} \psi(0^+) \\ \psi'(0^+) \end{pmatrix} = \begin{pmatrix} 1 & b' \\ 0 & 1 \end{pmatrix} \begin{pmatrix} \psi(0^-) \\ \psi'(0^-) \end{pmatrix}, \tag{4}$$

where b' is the coupling of this δ' interaction. It is clear that both definitions are different and, as mentioned in Chapters 2 and 3, we choose the definition introduced by Kurasov since both the δ and the δ' are compatible at the same point. In addition, the δ' interaction defined by Eq. (4) can not be interpreted as the derivative of the Dirac δ as its name could suggest [55]. This interaction is, however, used as such in Ref. [47] for analyzing the self-energy of a singular spherical shell. The interpretation as the derivative is more suitable for the δ' interaction used in this thesis, which was originally introduced as a distribution defined on the space of discontinuous functions[4] described in Ref. [53]. Nonetheless, in this thesis we are defining the δ' interaction by means of the matching conditions of Eq.(3), without using any properties regarding the derivative in the distributional sense.

As we have previously stated, most of the work for the δ-δ' was done in one dimension, on the basis of the original work [53]. A large part of it was developed by the theoretical physics group which I have been a part of during my Ph. D. [59–69]. This work was crucial for our task of proposing a generalization to hyperspherical geometries in the context of practical applications. For instance, one of the objectives was to consider geometries such that we can study one object inside another. In particular, in Chapter 1 we introduce H_d, the d-dimensional analogue of the operator H_1 in Eq. (2),

$$\begin{aligned} H_0 &:= -\frac{\mathrm{d}^2}{\mathrm{d}r^2} - \frac{d-1}{r}\frac{\mathrm{d}}{\mathrm{d}r} + \frac{\ell(\ell+d-2)}{r^2} + V_0(r), \\ H_d &:= H_0 + w_0\,\delta(r-r_0) + 2w_1\,\delta'(r-r_0). \end{aligned} \tag{5}$$

Note that we have also added a nonsingular potential $V_0(r)$. The introduction of this kind of potentials was also considered in some of the one-dimensional papers cited before [60, 62, 65, 66]. As we shall see, H_d determines a self-adjoint extension of H_0 when the proper domains are considered. In Chapter 1 we study only the singular interaction $V_0(r) = 0$, we add a spherical well inside the sphere in Chapter 2 and we consider the same spherical well plus the static Coulomb potential of a uniformly charged sphere of radius r_0 in Chapter 3. Along these chapters the changes produced due to the addition of new terms in the Hamiltonian are studied.

The main idea for generalizing the one-dimensional results is to consider the radial one-dimensional analogue. For a d-dimensional space, if we apply separation of variables for each value of the angular momentum ℓ in the dimensionless Schrödinger equation

$$[-\Delta + V(r)]\,\psi_\ell(\mathbf{x}) = E\psi_\ell(\mathbf{x}), \quad \psi_\ell(r,\Omega_d) = R_\ell(r)\mathcal{Y}_\ell(\Omega_d),$$

where $\mathcal{Y}_\ell(\Omega_d)$ is a combination of hyperspherical harmonics [70], we reduce the original problem to a one-dimensional one. Indeed, the radial function satisfies

$$\left[-\frac{\mathrm{d}^2}{\mathrm{d}r^2} - \frac{d-1}{r}\frac{\mathrm{d}}{\mathrm{d}r} + \frac{\ell(\ell+d-2)}{r^2} + V(r)\right] R_\ell(r) = H_d R_\ell(r) = E R_\ell. \tag{6}$$

[4] The standard theory with $C^\infty(\mathcal{D})$ functions fails since the second derivative with the Dirac delta and its derivative would not lead to a self-adjoint operator [53]. Nevertheless, D.J. Griffiths also arrived at the matching conditions of Eq. (3) integrating the one-dimensional Schrödinger equation [57], although there are some inconsistencies when the matching conditions for higher derivatives of the delta potential are derived [54, 58].

Introducing the reduced radial function $u_\ell(r) := r^{\frac{d-1}{2}} R_\ell(r)$ we have, essentially, a operator similar to H_1 in Eq. (2)

$$-\frac{\mathrm{d}^2}{\mathrm{d}r^2}+\frac{(d+2\ell-3)(d+2\ell-1)}{4r^2}. \tag{7}$$

In Chapters 2 and 3 we show how the matching conditions from the one-dimensional problem can be used for the reduced function, even though we have different domains and additional terms such as the centrifugal or centripetal ($d = 2$ and $\ell = 0$) potential in (7). With this analysis, we arrive at the following matching conditions for the radial function:

$$\begin{pmatrix} R_\ell(r_0^+) \\ R'_\ell(r_0^+) \end{pmatrix} = \begin{pmatrix} \alpha & 0 \\ \tilde{\beta} & \alpha^{-1} \end{pmatrix} \begin{pmatrix} R_\ell(r_0^-) \\ R'_\ell(r_0^-) \end{pmatrix}, \tag{8}$$

where the following parameters are obtained when undoing the changes introduced

$$\alpha := \frac{1+w_1}{1-w_1}, \quad \beta := \frac{w_0}{1-w_1^2}, \quad \tilde{\beta} := \beta - \frac{\left(\alpha^2-1\right)(d-1)}{2\,\alpha\, r_0} =: \frac{\tilde{w}_0}{1-w_1^2}. \tag{9}$$

Note that the matching conditions depend on the radius of the sphere and the spatial dimension. The dependence on d or r_0 does not appear in systems where the singular interaction is supported on a hyperplane of dimension $d-1 \geq 0$. In addition, the δ-δ' interaction also leads to boundary conditions. This can be proved analyzing the values $w_1 = \pm 1$, or equivalently[5], $b = \pm 2$ in Eq. (3). In this case, the matching conditions are not well defined and we have Robin and Dirichlet boundary conditions at each side [71]:

$$\begin{aligned} &R_{\lambda\ell}(r_0^+) - \frac{4}{\tilde{w}_0^+} R'_{\lambda\ell}(r_0^+) = 0, \qquad R_{\lambda\ell}(r_0^-) = 0 \quad \text{if} \quad w_1 = 1, \\ &R_{\lambda\ell}(r_0^-) + \frac{4}{\tilde{w}_0^-} R'_{\lambda\ell}(r_0^-) = 0, \qquad R_{\lambda\ell}(r_0^+) = 0 \quad \text{if} \quad w_1 = -1, \end{aligned} \tag{10}$$

where $\tilde{w}_0^\pm := w_0 \pm 2(1-d)/r_0$. The key point is that, within this approach, the problem of solving the Schrödinger equation with the singular interaction reduces to finding the solutions at each side of the interaction, matching them using Eq. (8). Note that if we choose a solvable potential $V_0(r)$, the wave function can be found analytically. In consequence, although we essentially have a one-dimensional problem for each value of the angular momentum, we are indeed modeling a three-dimensional system. This allows us to consider physical examples in the first part of the thesis. Apart from the application in QFT in Part II, in Chapters 2 and 3, we show how the low-lying nucleon energy levels of doubly magic nucleus like ^{208}Pb can be obtained. We consider neutrons in Chapter 2 and neutrons and protons in Chapter 3. In both chapters we compare these low-lying states with the ones obtained using the Woods-Saxon model, obtaining fair enough results in the range considered.

As we have mentioned, previous work with δ-δ' singular interactions was done essentially in one dimension. However, there are several works where the extension of this interaction to hyperspherical systems has been proposed, in particular [72, 73]. In Chapter 1 we explain why the results of the first article regarding the study of the

[5] The factor 2 multiplying the δ' coupling in Eq. (5) is introduced in order to have the values leading to boundary conditions at ± 1.

quantum mechanical potential are not as general as the ones proposed in this thesis. In short:

- The domain of the Hamiltonian considered, as proved in Chapter 2, should be square integrable functions satisfying

$$\{f(x) \in L^2(\mathbb{R}_{>0}) |\, H_0 f(x) \in L^2(\mathbb{R}_{>0})\}, \tag{11}$$

  instead of belonging to the Sobolev space $W_2^2(\mathbb{R}_{>0})$ as suggested in Ref. [72]. The latter is valid in one dimension since the function and its second derivative ($H_1 f$) should be square integrable but it is not the case for higher dimensions. Within these domains, it is clear that physical quantities like the finite value of the kinetic operator mentioned in Chapter 1 are finite. The latter can be easily proved using the Cauchy-Schwarz inequality.

- The matching conditions for the radial function written in Ref. [72] are given by Eq. (8) with $\beta = \tilde{\beta}$. These conditions are therefore independent of the radius and the dimension, being valid only for situations involving large values of r_0.

In addition, in Ref. [73] the matching conditions arising from constructing the most general self-adjoint extension are used. Omitting a global phase, these are simply given by

$$\begin{pmatrix} g_\ell(r_0^+) \\ g'_\ell(r_0^+) \end{pmatrix} = \begin{pmatrix} a_1 & b_1 \\ c_1 & d_1 \end{pmatrix} \begin{pmatrix} g_\ell(r_0^-) \\ g'_\ell(r_0^-) \end{pmatrix}, \tag{12}$$

where the determinant of the matching condition matrix should be equal to one. It is then clear that $b_1 = 0$ leads to the δ-δ' matching conditions. Performing the change $g(r) = r^{(2-d)/2}\varphi_\ell(r)$, it is stated that the new function $\varphi_\ell(r)$ satisfies

$$\begin{pmatrix} \varphi_\ell(r_0^+) \\ \varphi'_\ell(r_0^+) \end{pmatrix} = \begin{pmatrix} \bar{a}_1 & b_1 \\ \bar{c}_1 & d_1 \end{pmatrix} \begin{pmatrix} \varphi_\ell(r_0^-) \\ \varphi'_\ell(r_0^-) \end{pmatrix}, \tag{13}$$

being

$$\bar{a}_1 := a_1 + \frac{2-d}{2r_0} b_1, \qquad \bar{c} := c_1 + \frac{2-d}{2r_0} d_1. \tag{14}$$

However, performing the same change we find that the actual matching conditions should be

$$\begin{pmatrix} \varphi_\ell(r_0^+) \\ \varphi'_\ell(r_0^+) \end{pmatrix} = \begin{pmatrix} \bar{a} & \bar{b} \\ \bar{c} & \bar{d} \end{pmatrix} \begin{pmatrix} \varphi_\ell(r_0^-) \\ \varphi'_\ell(r_0^-) \end{pmatrix}, \tag{15}$$

being

$$\begin{aligned} \bar{a} &:= a_1 + \frac{(2-d)}{2r_0} b_1, \quad \bar{b} := b_1, \quad \bar{d} := d_1 + \frac{(d-2)}{2r_0} b_1, \\ \bar{c} &:= c_1 + \frac{(2-d)(2r_0(d_1 - a_1) + b_1(d-2))}{4r_0^2}. \end{aligned}$$

From these equations we find that the δ potential matching conditions, $a_1 = 1$, $d_1 = 1$ and $b_1 = 0$, are invariant under these changes and indeed the same for every dimension. This property was obtained also in the first chapter of the thesis [74], but it does not hold assuming Eq. (13) of [73].

As already mentioned, in all of these chapters special attention is paid to the quantum mechanical properties, like the bound state structure and phase shifts, which will be of central importance for Part II of the thesis. The main findings are briefly summarized here.

In Chapter 1, we focus on a hyperspherical singular interaction without a background potential $V_0(r) = 0$. We find the number of bound states for each value of the angular momentum and an upper bound as in Bargmann's inequalities [75]. We analyze the dependence on the spatial dimension d, paying special attention to the features of two-dimensional systems $d = 2$. Since we know the number of bound states is finite, we also find the maximum value of the angular momentum $\ell_{\max}$ such that bound states appear. This is particularly useful for Chapters 4 and 5, since $\ell_{\max} < 0$ implies that there are no bound states, which simplifies the calculation of the corresponding quantum energy when this potential is used in QFT. We also completely characterize the scattering states computing the phase shifts. As shown in the next section, this is essential for the interaction energy in Chapter 4 and the self-energy in Chapter 5. The zero-energy states and the mean value of the position operator are also studied.

In Chapter 2 we continue the analysis of the δ-δ' interaction including a spherical well. We show that some well known properties of continuous spherically symmetric potentials are fulfilled, characterizing also the unstable quantum states (resonances). We analyze the new features of the bound state structure, noting that, as expected, the singular interaction becomes less relevant if the well is deep enough. We also analyze large-parameter configurations, proving that the δ-δ' interaction vanishes in the limit $w_1 \to \pm\infty$, contrary to the delta potential strong limit, which leads to Dirichlet boundary conditions. This justifies why in Chapters 4 and 5 the interaction and self-energy tend to zero as $|w_1|$ goes to infinity. Now the analysis is more involved since we have, in addition to the modified Bessel functions of Chapter 1, Bessel functions of the first and second kind in the wave function. These functions present zeros in the positive real axis, giving rise to a richer structure for the bound states. In this chapter and in the following one, we have used a language that makes it suitable for the possible application in nuclear physics. Nevertheless, a nonrelativistic study of a quantum particle in a spherical well with a contact interaction in the edge can be analyzed within this framework as it is done in Chapter 1.

We conclude the analysis of this singular interaction in Chapter 3 adding the Coulombic term of a uniformly charged sphere of radius r_0

$$V_{\mathrm{C}}(r) = \frac{Ze^2}{4\pi\epsilon_0} \begin{cases} \dfrac{3-(r/r_0)^2}{2r_0}, & r \leq r_0, \\ \dfrac{1}{r}, & r > r_0, \end{cases}$$

where Z is the number of protons. As mentioned, this enables the study of neutron and proton energy states, thus completing the study of the previous chapter. It is worth mentioning that since we are adding new terms to the potential, the solution at each side of the interaction changes. In this case we essentially have confluent hypergeometric functions with complex arguments [76], which are less studied in the literature. Since the analytical results on the bound state structure are based on the properties of these special functions, the analysis is more involved. For instance, the secular equation is complex, although it can be proved using properties of Kummer's function that the imaginary part is meaningless. Nonetheless, we are able to find some analytical and numerical results regarding the spectrum and the role of the singular interaction. In particular, we emphasize here another advantage of considering the δ-δ' interaction rather than just the δ potential. In this paper we perform a phenomenological approach. Namely, within the proposed model the physical meaning of the Dirac δ is unequivocal, it accounts for the spin-orbit interaction. However, there is no clear interpretation of the δ' term. This is why we use this free parameter of the

model for finding the better fit with the available data, such as an optimized Woods-Saxon model [77]. We also check that the main structure and the role of the singular interaction are similar to the ones of the neutron case studied in Chapter 2, showing how we can use our model in order to work with actual physical constants.

We end this section emphasizing that in all of these three chapters some applications are indicated but they are circumstantial for the central objectives of this thesis. Although the usefulness in certain contexts has been proved, the main goal is to use this singular interaction as an intermediate step for obtaining relevant conclusions regarding the Casimir-Lifshitz effect in cavities. This is explained in the following section.

Singular interactions for scalar fields

As outlined in the previous paragraphs, the properties of the quantum mechanical model have been obtained from the stationary Schrödinger equation

$$[-\Delta + V(r)]\,\psi(\mathbf{x}) = E\psi(\mathbf{x}). \tag{16}$$

We now show why this study is also useful for the relativistic theory. In particular, as stated in Chapter 4, the dynamics of the quantum fluctuations of a massive scalar field φ interacting with a classical background $V(\mathbf{x})$ is governed by the action[6] [78]

$$\begin{aligned} S[\varphi] &= \int d^{3+1}x \left\{ \frac{1}{2}\,\partial_\mu\varphi\partial^\mu\varphi - F(\varphi) \right\}, \\ F(\varphi) &\coloneqq \frac{1}{2}\left(V(\mathbf{x})\varphi^2 + m^2\varphi^2\right). \end{aligned}$$

We are interested in the shift of the zero-point energy due to the presence of the background. Note that we are assuming that the background is adequately described by a classical theory so the scalar field interacts only with this background but not with other quantum fields. As already mentioned, this kind of procedure excludes the radiative corrections accounting the interaction with the electron-positron field. For instance, the analogue of the original Casimir effect is given by a massless field in which the background imposes Dirichlet boundary conditions at the plates [3]. Applying the variational principle, we arrive at the Klein-Gordon equation

$$\partial_\mu\partial^\mu\varphi(t,\mathbf{x}) + F'(\varphi(t,\mathbf{x})) = \partial_t^2\varphi(t,\mathbf{x}) - \Delta\varphi(t,\mathbf{x}) + F'(\varphi(t,\mathbf{x})) = 0, \tag{17}$$

where $F'(\varphi) \coloneqq \mathrm{d}F/\mathrm{d}\varphi$. For a static background it is convenient to apply the Fourier transform in time

$$\varphi(t,\mathbf{x}) = \int_{-\infty}^{\infty} d\omega\; \varphi_\omega(\mathbf{x})e^{-i\omega t}, \tag{18}$$

so we can work at a fixed frequency. The resulting equation can now be written as

$$[-\Delta + V(\mathbf{x})]\,\varphi_\omega(\mathbf{x}) = (\omega^2 - m^2)\varphi_\omega(\mathbf{x}). \tag{19}$$

Note that within QFT, the quantized field is considered as a collection of oscillators of all frequencies [79]. For each oscillator of frequency ω_n, the energy is given by[7]

$$E_n = \hbar\omega_n\left(n + \frac{1}{2}\right),$$

[6] We shall use units such that $\hbar = 1$ and $c = 1$.

[7] We have recovered Planck constant only for this formula and the next one.

where n is the eigenvalue of the number operator, the number of energy quanta. Consequently, the vacuum energy should be given by the sum of the zero-point energies of this set of oscillators:

$$E_0 = \frac{\hbar}{2}\sum_n \omega_n = \frac{\hbar}{2}\sum_n (k_n^2 + m^2)^{1/2}. \tag{20}$$

This expression is also referred to as the ground-state energy, being essentially the expectation value of the energy-density operator T^{00} in the vacuum state $|0\rangle$ [80]. This sum is obviously divergent and some process of regularization is needed. Nonetheless, regarding the connection between QM and QFT, we can see from Eqs. (16) and (19) that we have the same differential operator. It seems reasonable then that the previous nonrelativistic quantum mechanical analysis is relevant in this context. There are indeed more specific reasons justifying it. First, note that the definition of the δ-δ' interaction is the same as in QM. The construction of this potential is based on the self-adjoint extensions of a given operator, the Hamiltonian without the singular interaction, which is the same in both cases. However, the definition will be different for other fields. For instance, the analysis for the Dirac operator can be found in Ref. [81].

Second, we show how the self-energy is completely determined by the scattering data of the quantum mechanical potential. As we have mentioned, the energy in Eq. (20) needs to be regularized. For a comprehensive understanding of the connection between the operators in QM and QFT, it is convenient to see the details of the process of regularization. We can use the method based on spectral zeta functions explained in Chapter 5 and write

$$E_0(s) := \frac{\mu^{2s}}{2}\sum_{k\in C}(k^2+m^2)^{1/2-s} = \zeta_P(s-\frac{1}{2}), \qquad C := \{k \in \mathbb{R}_{>0} \mid f(k) = 0\}, \tag{21}$$

being μ a regularization parameter with dimensions of mass and $f(k)$ a function such that its zeros are the modes contributing to the zero-point energy, the mode-generating function introduced in the original works [82, 83]. This function determines the spectral zeta function ζ_P associated with the Schrödinger-type operator P of Eq. (19) [84]. For instance, for Dirichlet boundary conditions, this set can be found by requiring the field to be zero at the boundaries. Since we do not know the eigenvalues of the secular equation explicitly, we propose to evaluate the sum using Cauchy's argument principle. Note that we can write $f'(k)/f(k)$, which has simple poles at the modes such that $k \in C$ and the residue equals one at these points. The latter holds if we assume $f'(k) \neq 0$, which will be the case in the examples considered. As usual, we enclose the system in a large sphere of radius R and we impose Dirichlet boundary conditions on this auxiliary sphere. The final result is independent of the boundary conditions so we impose the simplest ones [3, 84]. Since we now have a bounded domain, the spectrum is discrete and the sum can be written as [85]

$$E_0(s) = \frac{\mu^{2s}}{2}\oint_\gamma \frac{dz}{2\pi i}(k^2+m^2)^{1/2-s}\frac{\mathrm{d}}{\mathrm{d}k}\log f(k), \tag{22}$$

where γ is a contour oriented counterclockwise on the complex plane such that it encloses all the values belonging to the set C. As mentioned, we have a Schrödinger-like equation with spherical symmetry so we know the solutions of the differential equation (19) from scattering theory. The radial part for large r is written in terms of

the Jost function $f_\ell(k)$ [86]

$$\rho_\ell(r) \sim f_\ell(k) h_\ell^{(2)}(kr) + f_\ell^*(k) h_\ell^{(1)}(kr). \tag{23}$$

That is to say, we have a term proportional to the spherical Hankel function of the first kind (outgoing) and the second kind (incoming). As mentioned before, we can obtain the secular equation imposing that the wave function[8] vanishes at the radius of the auxiliary sphere R. Consequently, we have

$$f(k) \coloneqq f_\ell(k) h_\ell^{(2)}(kR) + f_\ell^*(k) h_\ell^{(1)}(kR) = 0. \tag{24}$$

As in Casimir's original work [2], we now remove the infinite contribution from Minkowski free space. Due to the structure of the integrand, this is equivalent to consider the mode-generating function

$$f(k) \coloneqq \frac{f_\ell(k) h_\ell^{(2)}(kR) + f_\ell^*(k) h_\ell^{(1)}(kR)}{h_\ell^{(2)}(kR) + h_\ell^{(1)}(kR)}, \tag{25}$$

where the denominator is the free space term. The contour can be chosen such that half of it is just above the real axis and the other half just below it [3]. For the integration above the real axis, $f(z)$ reduces to $f_\ell(k)$ when the radius of the sphere goes to infinity. This is based on the asymptotic behaviour of Hankel functions, which can be found in Chapter 2. In the same way, when we make the radius of the sphere go to infinity for the integration contour below the real axis, $f(z)$ reduces to $f_\ell^*(k)$. We now use known properties of Jost functions from quantum mechanical scattering. From the Schwarz reflection principle, it can be proved that the Jost function satisfies $f_\ell(z) = f_\ell^*(-z^*)$ [86]. In particular,

$$f_\ell(x) = f_\ell^*(-x^*), \quad f_\ell(ix) = f_\ell^*(ix), \qquad x \in \mathbb{R}_{>0}. \tag{26}$$

Using the first relation it is clear that for the integration below the real axis, the integrand can be written as $f_\ell^*(k) = f_\ell(-k)$. With this, we now rotate to the imaginary axis. The integration contour over the real axis goes to the positive imaginary axis and the one below to the negative imaginary axis. Due to the symmetry properties of the Jost function mentioned, we can finally write [3]

$$E_0(s) = -\frac{\mu^{2s}}{2} \sum_{\ell \in \mathbb{N}_0} (2\ell + 1) \int_0^\infty \frac{\mathrm{d}\kappa}{2\pi i} (g(i\kappa) - g(-i\kappa)) \frac{\mathrm{d}}{\mathrm{d}\kappa} \log f_\ell(i\kappa), \tag{27}$$

where the degeneracy factor for three spatial dimensions $(2\ell + 1)$ has been included and

$$g(z) \coloneqq (z^2 + m^2)^{1/2-s}.$$

The function $g(i\kappa) - g(-i\kappa)$ should be evaluated considering the branch points of $g(z)$ at $z = \pm im$. Specifically, introducing polar coordinates

$$(z^2 + m^2)^{1/2-s} = ((z + im)(z - im))^{1/2-s}, \quad z \mp im \coloneqq r_\pm e^{i\theta_\pm},$$

[8] Note that the equations for the wave function and $\varphi_\omega(\mathbf{x})$ are the same but the interpretation of them are completely different. For instance, $\varphi_\omega(\mathbf{x})$ is simply a field evolving through a Schrödinger-like equation, with none of the probability interpretation of the wave function.

and taking into account the phases $\theta_\pm$, it is easily proved that

$$g(i\kappa) = \begin{cases} e^{i\pi(1/2-s)}(\kappa^2 - m^2)^{1/2-s} & \text{if} \quad \kappa > m, \\ 0 & \text{if} \quad \kappa \in (-m, m), \\ e^{-i\pi(1/2-s)}(\kappa^2 - m^2)^{1/2-s} & \text{if} \quad \kappa < -m. \end{cases} \tag{28}$$

Consequently, we can finally write

$$E_0(s) = -\frac{\mu^{2s}}{2\pi}\cos(\pi s)\sum_{\ell\in\mathbb{N}_0}(2\ell+1)\int_m^\infty \mathrm{d}\kappa(\kappa^2-m^2)^{1/2-s}\frac{\mathrm{d}}{\mathrm{d}\kappa}\log f_\ell(i\kappa). \tag{29}$$

As shown, the analysis of the first part of the thesis is crucial since, in the context of quantum fluctuations about classical configurations, the self-energy is completely determined by the Jost function of the quantum mechanical scattering problem. From the second equation of (26) we also note that this representation of the energy is real, as expected. In addition, the asymptotic behaviour $\kappa \to \infty$ of the integrand determines the lower bound of the strip of convergence and this region does not include $s = 0$ [84]. We then need to extend it in order to include this value. This can be achieved by adding and then subtracting the appropriate terms of the asymptotic behaviour, as explained in Chapter 5. Note also that the Jost function can be multiplied by a function which does not introduce new zeros, in particular for avoiding problems at the origin [84]. The zeta function regularization method also enables to isolate the divergences of the system. In particular, in Chapter 5 it is explained that for three spatial dimensions the divergence in the vacuum energy is proportional to the heat kernel coefficient a_2 [49]

$$E_0(s) = -\frac{a_2}{32\pi^2}\left(\frac{1}{s} + 2\log(\mu r_0)\right) + O(s^0). \tag{30}$$

This expression arises from the connection between the spectral zeta function and the heat kernel $K(t)$ through the Mellin transform

$$\zeta(s) = \int_0^\infty \mathrm{d}t\, \frac{t^{s-1}}{\Gamma(s)}K(t), \tag{31}$$

and the asymptotic small-t expansion of $K(t)$ in terms of the heat kernel coefficients [84]. In Chapter 5 we compute the self-energy of a δ-δ' sphere, finding a one-parameter family of couplings in which this energy is unambiguously defined since $a_2 = 0$. These couplings satisfy $c_0\lambda_1 = \lambda_0 r_0$ being

$$c_0 := \left(\frac{1}{24}\left(\sqrt[3]{42\sqrt{30}+224} - \frac{14^{2/3}}{\sqrt[3]{3\sqrt{30}+16}} + 14\right)\right)^{-1} \simeq 1.20818671192.$$

It is worth noting that for the δ potential $a_2 = 0$ if and only if $\lambda_0 = 0$, i.e., in the trivial configuration where the Casimir energy vanishes [49].

Furthermore, the analysis of the bound states is also important in this context. It is clear that the previous derivation is not valid if there exists a finite number of poles in the imaginary axis. From the quantum mechanical point of view, we know that poles in the positive imaginary axis can appear. Specifically, our potential is spherically symmetric so there exits a one-to-one correspondence between the bound states of the quantum mechanical Hamiltonian and the poles of the S matrix for each value of

the angular momentum [86]. In fact, this is the basis for Levinson's theorem. For each value of the angular momentum the components of the S matrix in the spherical basis are

$$s_\ell(k) = \exp(2i\delta_\ell(k)) = \frac{f_\ell(-k)}{f_\ell(k)}. \tag{32}$$

This is why we can also write the energy (29) in terms of the phase shifts δ_ℓ [3, 85, 87]. Leaving aside the domains of analyticity, we can intuitively show that zeros of $f_\ell(k)$ give rise to bound states. If k_0 satisfies $f_\ell(k_0) = 0$, from Eq. (23) we have

$$\rho_{\omega,\ell}(r) \sim f_\ell(-k_0) h_\ell^{(1)}(kr). \tag{33}$$

Due to the asymptotic behaviour of Hankel functions shown in Chapter 2, we have an exponentially decreasing behaviour. Taking into account the regularity condition of the wave function at the origin we have a square integrable solution, i.e., a bound state. In consequence, the quantum mechanical Hamiltonian admits an eigenstate of energy $k_0/2m$ and for these cases we should change the contour of integration. This would give rise to an expression similar to (29) but with the Cauchy principal value and a finite number of terms accounting for the residues at the positive imaginary axis. In the corresponding chapters, we restrict ourselves to cases in which there are no bound states, not discussing any questions related to vacuum decay and particle creation [79]. For determining the values of the couplings such that this occurs we use the analysis of the bound state structure of Part I. In particular, we can always determine in which regions of the space of couplings $\{w_0, w_1\}$ there are bound states for a given value of the angular momentum. For that we use the maximum value of the angular momentum given in Chapter 1

$$\ell_{\max} := \lfloor L_{\max} \rfloor, \qquad L_{\max} := \frac{w_1 - x_0\, w_0/2}{w_1^2 + 1} + \frac{2-d}{2}, \tag{34}$$

since we know that $L_{max} < 0$ implies the nonexistence of bound states.

So far we have proved the usefulness of the quantum mechanical analysis for the self-energy. However, the first part of the thesis also plays a crucial role for determining the interaction energy. If the spatial support of the two bodies satisfies $\operatorname{supp} V_1 \cap \operatorname{supp} V_2 = \emptyset$, the vacuum interaction energy between the two objects can be written as [19, 20]

$$E_{\text{int}} = \frac{1}{2\pi} \int_0^\infty \mathrm{d}\kappa \, \operatorname{Tr} \log\left(\mathbb{I} - \mathbb{T}_1 \mathbb{G}_{12}^0 \mathbb{T}_2 \mathbb{G}_{21}^0\right), \tag{35}$$

where the integration is over imaginary frequencies $\omega = i\kappa$. This is why the name TGTG representation is used. It is worth mentioning that this representation can also be derived following a mode summation approach similar to the one explained here for the self-energy, starting with Eq. (20) but with a different set C [88, 89]. Contrary to the Casimir energy of a single object, the interaction energy always gives an unambiguous finite result for the force. The idea behind it lies in the independence of the heat kernel coefficients, which determine the divergences, on the distance between bodies [3]. Note that the properties of each body are given by the corresponding Lippmann-Schwinger $\mathbb{T}_i$ operator and the relative position between both objects enters through the operator $\mathbb{G}_{ij}^0$, related to the projection of the propagator across the vacuum $\mathbb{G}^0$. Consequently, with this representation, the properties of each body and the distance between their centers can be treated separately. We then focus on the

transition matrices, since for concentric spheres $\mathbb{G}_{ij}^0$ are essentially identities[9]. When the two objects are outside each other we need the usual components of the $\mathbb{T}_i$ operator in nonrelativistic quantum mechanics. Specifically, if φ^{reg} represents a regular wave, in spherical coordinates the radial part is given by the Bessel function of the first kind, we need the components $\langle \varphi^{\text{reg}}, \mathbb{T}_i \varphi^{\text{reg}} \rangle$. From QM we know the radial solution inside and outside the sphere, which can be written as

$$\rho_\ell(r) = \begin{cases} A_\ell \rho_\ell^{\text{reg}}(r) & r < r_0, \\ a_\ell \rho_\ell^{\text{reg}}(r) + b_\ell \rho_\ell^{\text{out}}(r) & r > r_0. \end{cases} \tag{36}$$

Consequently, the scattering produced by the sphere in this situation can be calculated with the components

$$T_i^\ell = -\frac{b_\ell}{a_\ell}. \tag{37}$$

This is the ratio between the scattered component, proportional to the outgoing wave, and the incident wave, proportional to the regular wave. Due to the relation between the T matrix and the S matrix we have [19, 90]

$$T_i^\ell = -\frac{b_\ell}{a_\ell} \propto \exp(2i\delta_\ell(k)) - 1. \tag{38}$$

That is to say, we can compute the components of $\mathbb{T}_i$ entering in the TGTG operator with the scattering analysis performed in the first part of the thesis. As stated above, we are going to focus on interior configurations. That is, systems of two objects in which one of them is inside the other without overlapping. In this case, we require different components for $\mathbb{T}_2$ in (35). This is proved in Ref. [20, 88] and explained in the second part of the thesis. Nonetheless, this case can also be analyzed from a quantum mechanical perspective. The components of $\mathbb{T}_2$ appearing when the first object is inside the second can be computed if we investigate a scattering experiment in which the source and the detector are inside the cavity. The solution in this case can be written as

$$\rho_\ell(r) = \begin{cases} \tilde{a}_\ell \rho_\ell^{\text{reg}}(r) + \tilde{b}_\ell \rho_\ell^{\text{out}}(r) & r < r_0, \\ B_\ell \rho_\ell^{\text{out}}(r) & r > r_0. \end{cases} \tag{39}$$

The components of $\mathbb{T}$ are then given by the ratio of the reflected and the emitted wave, but this time inside the sphere,

$$\widetilde{T}_2^\ell = -\frac{\tilde{a}_\ell}{\tilde{b}_\ell}. \tag{40}$$

This atypical scattering experiment is less studied in the literature and some differences with respect to the regular setup will be drawn in Chapter 4 for two concentric δ-δ' spheres.

Casimir-Lifshitz effect in cavity configurations

With all of these findings, in Chapter 4 we analyze how the signs of the couplings of the singular potentials determine the positive or negative value of the interaction energy. In particular, along this chapter we denote the couplings by $\{\lambda_{0,i}, \lambda_{1,i}\}_{i=1,2}$,

[9] This is one of the few cases, together with the planar geometry, in which both $\mathbb{T}$ and $\mathbb{G}_{ij}^0$ are simultaneously diagonal in the appropriate basis.

being the two spheres modeled by

$$V(r) = V_1(r) + V_2(r) = \sum_{i=1}^{2} \lambda_{0,i}\delta(r - r_i) + 2\lambda_{1,i}\delta'(r - r_i), \quad r_1 < r_2. \tag{41}$$

In Chapter 4 we show the sign of the interaction energy for two different configurations, which for clarity we reproduce again here in Figs. 1a and 1b. With this numeri-

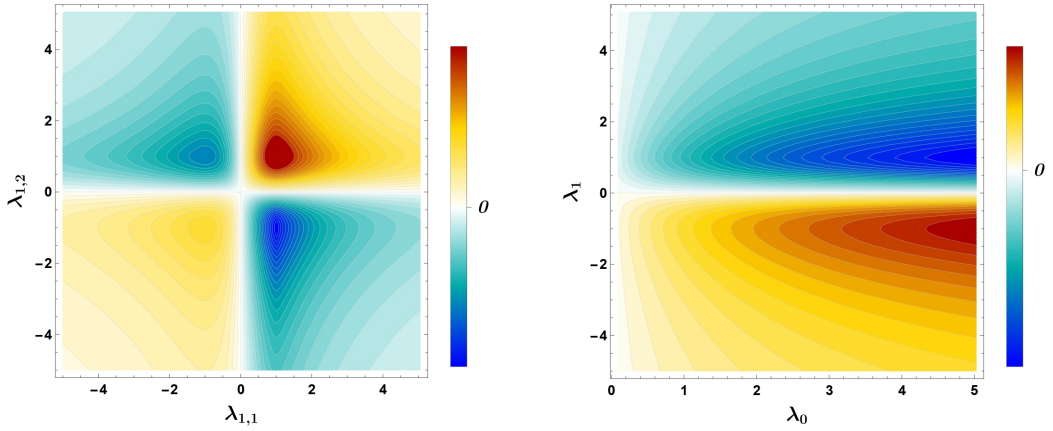

(a) Interaction energy between two concentric δ' spheres ($\lambda_{0,1} = 0 = \lambda_{0,2} = 0$).

(b) Interaction energy between a δ and a δ' sphere ($\lambda_{1,1} = 0$ and $\lambda_{0,2} = 0$).

Figure 1: Dependence of the interaction energy on the sign of the couplings.

cal analysis, we show that the signs of λ_0 and, in particular, λ_1 determine the sign of the interaction energy. Indeed, for δ spherical shells only positive values are obtained, since $\lambda_{0,i} > 0$ is assumed in order to avoid bound states in the quantum mechanical sense. Furthermore, this behaviour is not a particular feature of spherical geometry and for parallel plates the same pattern was found in Ref. [63]. Although the field can be obtained analytically, the interaction energy (35) can only be evaluated numerically. In view of this, our aim was to generalize these results to more realistic systems with the electromagnetic field. In addition, due to the reasons that we will explain below, we tried to obtain analytic results on the sign without performing the explicit calculation.

First, note that if we assume that the coupling of the electromagnetic field to matter can be described by continuous permittivity ε and permeability μ functions, for a homogeneous medium characterized by ε_M and μ_M, Maxwell curl equations, can be written as a stationary vector Schrödinger-like equation

$$[\boldsymbol{\nabla} \times \boldsymbol{\nabla} \times + \mathbb{V}(\omega, \mathbf{x})]\, \mathbf{E}(\omega, \mathbf{x}) = k^2 \mathbf{E}(\omega, \mathbf{x}).$$

We have defined $k := \sqrt{\varepsilon_M}\omega$ and the potential $\mathbb{V}(\omega, \mathbf{x})$, now a differential operator:

$$\mathbb{V}(\omega, \mathbf{x}) := \mathbb{I}\omega^2 \left[\varepsilon_M(\omega) - \varepsilon(\omega, \mathbf{x})\right] + \boldsymbol{\nabla} \times \left[\frac{1}{\mu(\omega, \mathbf{x})} - \frac{1}{\mu_M(\omega)}\right] \boldsymbol{\nabla} \times . \tag{42}$$

As for the scalar case, we can write the interaction energy with an analogous representation [19, 20]

$$E_{\text{int}} = \frac{1}{2\pi} \int_0^\infty \mathrm{d}\kappa \, \mathrm{Tr} \log\left(\mathbb{I} - \mathbb{T}_1 \mathbb{G}_{12}^M \mathbb{T}_2 \mathbb{G}_{21}^M\right). \tag{43}$$

The properties of each body are also encoded in the Lippmann-Schwinger $\mathbb{T}$ operator, now being [91]

$$\mathbb{T}_i = \mathbb{V}_i \left(\mathbb{I} + \mathbb{G}^M \mathbb{V}_i \right)^{-1} : \mathcal{H}_i \to \mathcal{H}_i \coloneqq L^2(\operatorname{supp} \mathbb{V}_i)^3.$$

Furthermore, the relative position between both objects enters through the operator $\mathbb{G}^M_{ij} \coloneqq \mathbb{P}_i \mathbb{G}^M \mathbb{P}_j : \mathcal{H}_j \to \mathcal{H}_i$, being $\mathbb{G}^M$ the propagator across the medium and $\mathbb{P}_i$ the projection operator onto the Hilbert space $\mathcal{H}_i$. In particular, for spherically symmetric systems the problem reduces to two scalar problems, one for each polarization [92]. For instance, the transverse electric (TE) potential of a dielectric sphere is [93]

$$V^{\mathrm{TE}}(\omega, r) = \omega^2 \left[\varepsilon_M(\omega) - \varepsilon_1(\omega, r) \right].$$

The main differences with respect to the scalar case are that we do not have the $\ell = 0$ contribution and the frequency (energy) dependence on the potential. In any case, the sign of the potential $\mathbb{V}_i$ describing each body is determined by the following relation for the relative permittivities and permeabilities:

$$s_i \coloneqq \operatorname{sgn} \mathbb{V}_i = \pm 1 \quad \text{if} \quad \varepsilon_i(i\kappa, \mathbf{x}) \gtrless \varepsilon_M(i\kappa) \quad \text{and} \quad \mu_i(i\kappa, \mathbf{x}) \lessgtr \mu_M(i\kappa), \tag{44}$$

for every frequency and the whole body [23]. Within this context, in the two final chapters we are able to rewrite the TGTG operator inside the integral in a suitable way and, using some results of classical scattering theory, we arrive at the main findings of this thesis. In particular, for the configurations considered $s_i \mathbb{T}_i$ is a positive operator so we can write $\mathbb{T}_i = s_i \sqrt{s_i \mathbb{T}_i} \sqrt{s_i \mathbb{T}_i}$, being $\sqrt{s_i \mathbb{T}_i}$ the square root of $s_i \mathbb{T}_i$. In consequence, the interaction energy can be rewritten as

$$E_{\mathrm{int}} = \frac{1}{2\pi} \int_0^\infty \mathrm{d}\kappa \operatorname{Tr} \log(\mathbb{I} - s\, \mathbb{M}_i), \tag{45}$$

where we have defined $s \coloneqq s_1 s_2$ and

$$\mathbb{M}_1 \coloneqq \sqrt{s_2 \mathbb{T}_2} \mathbb{G}^M_{21} s_1 \mathbb{T}_1 \mathbb{G}^M_{12} \sqrt{s_2 \mathbb{T}_2} = (\sqrt{s_1 \mathbb{T}_1} \mathbb{G}^M_{12} \sqrt{s_2 \mathbb{T}_2})^\dagger \sqrt{s_1 \mathbb{T}_1} \mathbb{G}^M_{12} \sqrt{s_2 \mathbb{T}_2},$$
$$\mathbb{M}_2 \coloneqq \sqrt{s_1 \mathbb{T}_1} \mathbb{G}^M_{12} s_2 \mathbb{T}_2 \mathbb{G}^M_{21} \sqrt{s_1 \mathbb{T}_1} = (\sqrt{s_2 \mathbb{T}_2} \mathbb{G}^M_{21} \sqrt{s_1 \mathbb{T}_1})^\dagger \sqrt{s_2 \mathbb{T}_2} \mathbb{G}^M_{21} \sqrt{s_1 \mathbb{T}_1},$$

where † stands for the adjoint operation. In Chapter 6 we use Eq. (45) for $i = 1$ and the same formula with $i = 2$ in Chapter 7. Once the expressions are written as above, we can make use of standard manipulations like

$$\langle \mathbf{E}, \mathbb{A}^\dagger \mathbb{A} \mathbf{E} \rangle = \langle \mathbb{A}\mathbf{E}, \mathbb{A}\mathbf{E} \rangle = \|\mathbb{A}\mathbf{E}\|^2 \geq 0 \tag{46}$$

for determining the sign of the energy. Indeed, we easily prove that the sign of the interaction energy is given by $\operatorname{sgn} E_{\mathrm{int}} = -s$. The latter holds for two arbitrary magnetodielectrics, even if they lie outside each other, as long as there is no overlapping.

We then proceed to study the pressure acting on the spherical surfaces of the systems shown in Figs. 2a and 2b. To define this pressure we do not need to include elastic deformations and we simply make use of the principle of virtual work. Accordingly, the mean value of the pressure due to a virtual variation of the radius satisfies [94, 95]

$$\langle p_{\mathrm{int}} \rangle \coloneqq \frac{1}{4\pi} \int_{S^2} \mathrm{d}\Omega\, p_{\mathrm{int}}(r, \Omega) = -\frac{1}{4\pi r^2} \frac{\partial E_{\mathrm{int}}}{\partial r}. \tag{47}$$

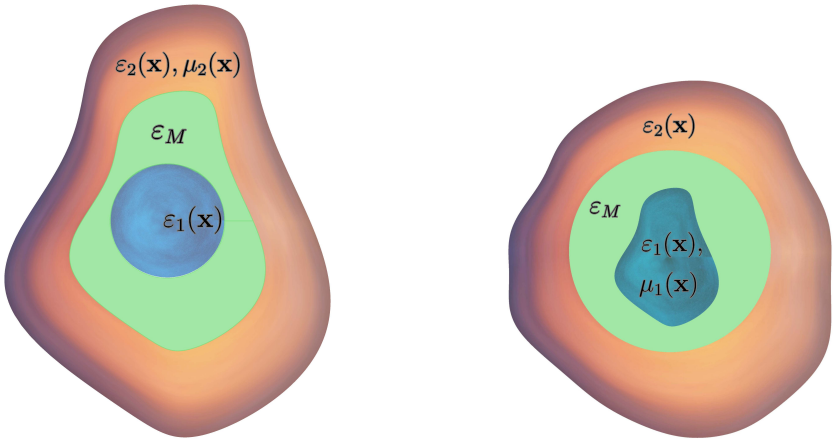

(a) Configuration studied in Chapter 6. (b) Configuration studied in Chapter 7.

Figure 2: Cross-section view of the systems under study in the last two chapters.

In order to find the derivative with respect to the radius of the interaction energy, in Chapter 6 we employ the quantum mechanical Calogero equation [96] generalized to electromagnetic scattering by arbitrarily shaped objects [97, 98]. Adapted to imaginary frequencies with the definitions given in Chapter 7, the derivative of $\mathbb{T}^{\text{ext}}$ defined in Chapter 6 can be written as

$$\partial_r \mathbb{T}^{\text{ext}} = \kappa \mathbb{W}^{\dagger}_{\text{ext}}(r) \mathbb{U}(r) \mathbb{W}_{\text{ext}}(r), \tag{48}$$

where $\mathbb{T}^{\text{ext}}$ are the components of the $\mathbb{T}$ operator in the spherical wave basis. Due to the structure of previous equation, we can again make use of standard manipulations with the adjoint operator for determining the sign of the pressure. As in the scalar case, different components enter in the calculation for the second body, corresponding to a different scattering experiment. Since fewer articles on this topic can be found in the literature, some new results were developed. Specifically, in Chapter 7 we prove the following nonlinear differential equation for the interior components of the T matrix

$$\partial_r \mathbb{T}^{\text{int}} = -\kappa \mathbb{W}^{\dagger}_{\text{int}}(r) \mathbb{U}(r) \mathbb{W}_{\text{int}}(r). \tag{49}$$

The derivation follows from the Lippmann-Schwinger equation for a scattering experiment in which the source and the detector are inside the cavity[10]. Due to this different setup, an additional global minus sign appears compared with the usual case (48). With this, we are then able to determine the sign of the interaction pressure acting on the two spherical surfaces shown in Figs. 2a and 2b

$$\operatorname{sgn} E_{\text{int}} = -\operatorname{sgn} \langle p_{\text{int}} \rangle_{\text{sphere}} = \operatorname{sgn} \langle p_{\text{int}} \rangle_{\text{cavity}} = -s_1 s_2. \tag{50}$$

This is one of the main results of the thesis. As we can see, the sign of the interaction energy completely determines the sign of the pressure on the spherical surfaces. Although the latter also holds for planar geometries under general assumptions [17], it is not always the case and, for example, attractive and repulsive forces can be found for negative energies only [31]. The equations in (50) are also independent of the geometry and matter distribution of the bodies as long as the signs s_i are well defined. We have considered inhomogeneous permittivity functions $\varepsilon(i\kappa, \mathbf{x})$ such that the sign

[10] We also consider the other two possibilities, source (detector) inside and detector (source) outside.

of $\varepsilon_i(i\kappa, \mathbf{x}) - \varepsilon_M(i\kappa)$ is independent of κ and $\mathbf{x}$ and we can write

$$s_i = \operatorname{sgn}(\varepsilon_i - \varepsilon_M) = \operatorname{sgn}[\varepsilon_i(i\kappa, \mathbf{x}) - \varepsilon_M(i\kappa)]. \tag{51}$$

In addition, we can always consider a magnetodielectric object for the cavity in the first system (Fig. 2a) and for the inner object in the second system (Fig. 2b). The sign of the potential is now determined by Eq. (44) with $\mu_M = 1$. As shown in Chapters 6 and 7, we can also extend the result of Eq. (50) to systems at thermal equilibrium since the free energy $\mathcal{F}_{\text{int}}$ satisfies [80]

$$\langle p_{\text{int}}(T) \rangle = -\frac{1}{4\pi r_0^2} \frac{\partial \mathcal{F}_{\text{int}}(T)}{\partial r_0}, \tag{52}$$

and we can perform a similar derivation computing $\mathcal{F}_{\text{int}}(T)$ replacing the integral in E_{int} by a sum over the Matsubara frequencies $2\pi k_{\text{B}} n T$, where the zero mode is weighted by $1/2$ [3]. The key point is that our analysis holds for each fixed frequency.

As already mentioned, the self-energy contribution should also be considered when computing the pressure since the interaction term has no independent meaning. In Chapter 6 we include the self-energy contribution for one of the cases in which it is unambiguously defined. As explained in Chapter 5, if the corresponding heat kernel coefficient does not vanish for a massless field when the whole space and both polarizations are taken together, there is in general no satisfactory interpretation of the self-energy [3]. Unfortunately, there are a few cases in which this occurs, being most of them listed in the introduction of Chapter 5 and Ref. [99]. A dilute dielectric ball is one of the examples, where the renormalized energy takes the form

$$E_1^{\text{ren}} = \frac{23}{1536\pi r_1} (\varepsilon_1 - 1)^2 + O(\varepsilon_1 - 1)^3. \tag{53}$$

For this case we find situations in which the total pressure is repulsive, tending to expand the sphere inside the cavity.

Despite that, the findings described in Chapters 6 and 7 can be checked against experimentally verified results. In particular, note that the sign for the interaction force found by DLP in 1961 [14] is determined in a similar way as described here for the interaction pressure. In particular, assuming that expression (1) holds for every frequency, this relation can be written in terms of the signs of the potentials as

$$-\operatorname{sgn}[\varepsilon_1(i\kappa) - \varepsilon_M(i\kappa)] \operatorname{sgn}[\varepsilon_2(i\kappa) - \varepsilon_M(i\kappa)] = -s_1 s_2,$$

and the DLP configuration can be recovered with the systems of Figs. 2a and 2b. Specifically, if we consider the configuration shown in Fig. 3 and we take the radii of the sphere and cavity wall to infinity, keeping the difference between them constant [100], we arrive at the planar geometry with three slabs [14]. Indeed, it is a generalization of the original configuration since we do not assume homogeneous permittivities, but functions depending on the coordinate perpendicular to the slabs. Now, the DLP result on the sign of the force per unit area $\operatorname{sgn} F_{\text{int}}$ can be found from Eq. (50), noting

$$\operatorname{sgn} F_{\text{int}} = -\operatorname{sgn} \partial_d E_{\text{int}} = -\operatorname{sgn} \partial_{r_2} E_{\text{int}} = \operatorname{sgn} \partial_{r_1} E_{\text{int}}, \tag{54}$$

where $d := r_2 - r_1 > 0$ is the difference between the radii of the cavity wall and the sphere. From the previous equation, it is clear why the minus sign of Eq. (49) is essential for obtaining consistent results. A particular choice of materials in which

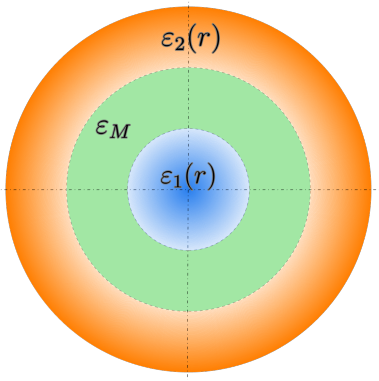

Figure 3: Cross-section view of the particular case which leads to the DLP result.

F_{int} is repulsive is proposed in the experiment described in Ref. [15], where they used a sphere coated with gold and a silica plate immersed in bromobenzene, being

$$-(\varepsilon_{\text{g}}(i\kappa)-\varepsilon_{\text{b}}(i\kappa))(\varepsilon_{\text{s}}(i\kappa)-\varepsilon_{\text{b}}(i\kappa))>0, \tag{55}$$

for a given range of frequencies, as shown in Fig. 4. Indeed, this relation only needs to be valid for the frequencies contributing most to the integral [23]. Note also that from

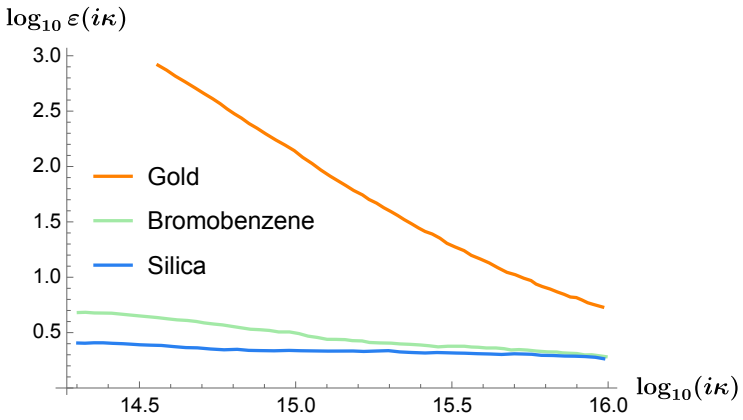

Figure 4: Analytic continuation of $\varepsilon(\omega)$ for the materials used in Ref. [15]. The frequency is given in rad/s.

Kramers–Kronig relations, we can write the analytic continuation of the dielectric permittivity to the imaginary axis in terms of $\varepsilon(\omega)$ as [3]

$$\varepsilon(i\kappa)=1+\frac{2}{\pi}\int_0^\infty \mathrm{d}\omega\frac{\omega\,\mathrm{Im}\,\varepsilon(\omega)}{\omega^2+\kappa^2},$$

from which it is clear that $\varepsilon(i\kappa)$ is a real quantity along the positive imaginary frequency axis [101]. It is also worth mentioning that in systems like the one shown in Fig. 3, the interaction force acting on each object vanishes due to symmetry reasons. In fact, this happens for any system which is invariant under mirror symmetry with respect to the three spatial planes, like the one shown in Chapter 6. However, the pressure is not zero and it should be taken into account for systems such as those composed of liquid dielectrics, although other effects, such as hydrodynamic forces, should also be considered [37, 38].

We conclude this introduction to the main results emphasizing that we have been

able to obtain the sign of the pressure for the systems described in Figs. 2a and 2b without relying on any particular symmetric configuration, in which the calculation could be feasible. This is due to the scattering approach, which was previously employed in the seminal works on the attractive character of the force [21] and the study of stable levitation based on Casimir-Lifshitz forces [23]. However, the main difference with respect to these articles is that we vary the interaction energy with respect to the radii of the sphere and cavity wall and not with respect to the distance between the bodies. In consequence, we do not study the properties of the propagators with respect to this distance but the variation of the transition matrices with respect to the radius. This is why we need particular results of classical electromagnetic scattering. In fact, we have developed them for situations in which the source or the detector can be inside the cavity. Note that this is not particularly useful in classical electrodynamics since in current experiments both are outside the target, but it is needed for studying the interaction energy when one object is contained within another. Since we only focus on the radial dependence, we can assume an arbitrarily shaped geometry, an inhomogeneous matter distribution and nontrivial permeabilities for the nonspherical object. Despite this difference with the two theorems aforementioned, we obtain similar results. For instance, the stability reached with Casimir-Lifshitz forces is also completely determined by the product of the signs of the potentials s_i, leading, in general, to unstable equilibrium [23].

Structure of the thesis and methodology employed

This thesis comprises several self-contained topics that are connected by the general framework described above. It is written as a compendium of publications and seven scientific papers have been included [74, 100, 102–106], being one of them pending of acceptance [106]. Since each chapter adapts the corresponding article, it is self-explanatory with its own bibliography, although some minimal changes with respect the original papers have been included for ease of reading of the whole thesis. This thesis also fulfills the requirements to obtain the degree of Doctor of Philosophy in Physics with the International Mention from the University of Valladolid.

The methods used within this thesis are mostly analytical. The remaining numerical and graphical calculations are done within the Wolfram Language using the program Mathematica. We have also used the interpreted programming language Python in Chapter 5 for the numerical integral and sum of the finite energy E_0^{fin}. The work presented is divided into two parts, being each of them organized as follows:

Part I: Study of spherical δ-δ' interactions

- Chapter 1. **Hyperspherical δ-δ' potentials**

  Adapted from: J. M. Muñoz-Castañeda, L. M. Nieto and C. Romaniega, *Hyperspherical δ-δ' potentials*, Ann. Phys. **400**, 246 (2019).

  In this first chapter the spherical δ-δ' interaction for a d-dimensional space is defined. The bound states, scattering states and zero-energy states are computed. As stated above, these results will play a central role in the second part of this thesis.

- Chapter 2. **Regular and δ-δ' potentials I**

  C. Romaniega, M. Gadella, R. M. Id Betan and L. M. Nieto, *An approximation to the Woods–Saxon potential based on a contact interaction*, Eur. Phys. J. Plus **135**, 372 (2020).

We now add a spherical well to the potential, extending the study of the singular interaction defined in the previous chapter using von Neumann's theory. We show how we can adapt the one-dimensional work [53] to our system with singular and regular spherical potentials. We also characterize and calculate the number of bound states, extend some properties of continuous spherically symmetric potentials and describe the unstable quantum states. We indicate the possible use of the interaction as a first approximation of real physical systems, particularly for describing neutron energy levels for double magic nuclei.

- Chapter 3. **Regular and δ-δ' potentials II** .

  A. Martín-Mozo, L. M. Nieto and C. Romaniega, *A solvable contact potential based on a nuclear model*, Eur. Phys. J. Plus **137**, 33 (2022).

  In this chapter we continue the analysis of the previous one. We now add the static Coulomb potential of a uniformly charged sphere. This enables the study of proton energy states and, as in the previous paper, some applications for describing physical systems are indicated. These are based on the properties of confluent hypergeometric functions with complex arguments. In addition, we now find the optimal δ' contribution which best fits the available data for the nucleon level schemes of the nuclei ^{208}Pb, ^{40}Ca and ^{16}O.

Part II: Casimir-Lifshitz energy and pressure in cavities

- Chapter 4. **Interaction energy between two concentric δ-δ' spheres**.

  I. Cavero-Peláez, J. M. Muñoz-Castañeda, and C. Romaniega, *Casimir energy for concentric δ-δ' spheres*, Phys. Rev. D **103**, 045005 (2021).

  We begin the second part studying the interaction energy of a massless scalar field in the presence of two concentric δ-δ' spheres. As indicated, some results from the previous part of the thesis are needed. In particular, we have computed the interaction energy for the values of the potential such that there are no bound states in the quantum mechanical sense. In addition, the components of the $\mathbb{T}$ operators appearing in the representation of the interaction Casimir energy in terms of functional determinants are completely determined using the scattering data computed in the first part of the thesis.

- Chapter 5. **Self-energy of a δ-δ' sphere**.

  C. Romaniega, I. Cavero-Peláez, and J. M. Muñoz-Castañeda, *Casimir self-energy of a δ-δ' sphere* (pending of acceptance).

  We continue the analysis of the previous chapter computing the self-energy contribution to the pressure on a δ-δ' sphere using the zeta function regularization method. In this context, the energy is completely determined by the Jost function for each value of the angular momentum, which is easily found with the scattering phase shifts of the first part of the thesis. We find a simple relation between the couplings of the δ and δ' interactions such that the Casimir self-energy is unambiguously defined, computing the relevant heat kernel coefficient. We also check our results against particular cases previously studied in the literature.

- Chapter 6. **Casimir-Lifshitz pressure in cavities I** .

  C. Romaniega, *Repulsive Casimir–Lifshitz pressure in closed cavities*, Eur. Phys. J. Plus **136**, 327 (2021).

In these two final chapters we study the interaction term of the energy for the electromagnetic field in the presence of more realistic bodies. Specifically, in this chapter we consider a dielectric sphere enclosed within an arbitrarily shaped magnetodielectric cavity. We determine, under general hypotheses, the sign of the interaction energy and pressure acting on the sphere. This is achieved by rewriting the expression in terms of functional determinants and analyzing the properties of the classical T matrices. In this sense, this approach is similar to the one employed in Refs. [21, 23]. In addition, in this chapter and in the following we also obtain the Dzyaloshinskii-Lifshitz-Pitaevskii result [14] on the sign of the interaction force as a limiting case. For a dilute dielectric ball we also include the self-energy contribution, obtaining a total repulsive pressure.

- Chapter 7. **Casimir-Lifshitz pressure in cavities II** .

  C. Romaniega, *Casimir-Lifshitz pressure on cavity walls*, Eur. Phys. J. Plus **136**, 1051 (2021).

  We continue the analysis of the previous chapter, now considering a dielectric object with a spherical cavity in which another arbitrarily shaped magnetodielectric object is enclosed. Due to the components of the $\mathbb{T}$ operator entering in the TGTG representation, we need to introduce some novel results of classical electromagnetic scattering for configurations with the source and detector inside the cavity. The latter is based on the Lippmann-Schwinger equation and an invariant imbedding procedure. As in the previous chapter, the results on the energy and pressure are generalized to finite temperature systems at thermal equilibrium. We also check against particular examples found in the literature like conducting shells and homogeneous spherical dielectrics.

  The structures of this chapter and the previous one are very similar. We have exploited the derivation of Chapter 6, introducing the corresponding modifications needed for the study of the new configuration and a slightly different notation for some intermediate steps.

References for Introduction

[1] P. W. Milonni and M. L. Shih, Contemp. Phys. **33**, 313 (1992).

[2] H.B.G. Casimir, Front. Phys. **100**, 61 (1948).

[3] M. Bordag, G. L. Klimchitskaya, U. Mohideen, and V. M. Mostepanenko, *Advances in the Casimir Effect* (Oxford University Press, Oxford, 2009).

[4] M. Bordag, D. Robaschik, and E. Wieczorek, Ann. Phys. **165**, 192 (1985).

[5] E. M. Lifshitz, Sov. Phys. JETP **2**, 73 (1956).

[6] H.B.G. Casimir and D. Polder, Phys. Rev. **73**, 360 (1948).

[7] H.B.G. Casimir, Physica **19**, 846 (1953).

[8] T. H. Boyer, Phys. Rev. **174**, 1764 (1968).

[9] B. Davies, J. Math. Phys. **13**, 1324 (1972).

[10] R. Balian and B. Duplantier, Ann. Phys. **104**, 300 (1977).

[11] R. Balian and B. Duplantier, Ann. Phys. **112**, 165 (1978).

[12] K. A. Milton, L. L. DeRaad Jr, and J. Schwinger, Ann. Phys. **115**, 388 (1978).

[13] L. L. DeRaad Jr and K. A. Milton, Ann. Phys. **136**, 229 (1981).

[14]I. E. Dzyaloshinskii, E. M. Lifshitz, and L. P. Pitaevskii, Adv. Phys. **10**, 165 (1961).

[15]J. N. Munday, F. Capasso, and V. A. Parsegian, Nature (London) **457**, 170 (2009).

[16]D. Dalvit, P. Milonni, D. Roberts, and F. Da Rosa, *Casimir Physics*, Vol. 834 (Springer-Berlin, Heidelberg, 2011).

[17]M. Asorey and J. M. Munoz-Castaneda, Nucl. Phys. B **874**, 852 (2013).

[18]M. Asorey, D. Garcia-Alvarez, and J. M. Munoz-Castaneda, J. Phys. A **39**, 6127 (2006).

[19]O. Kenneth and I. Klich, Phys. Rev. B **78**, 014103 (2008).

[20]S. J. Rahi, T. Emig, N. Graham, R. L. Jaffe, and M. Kardar, Phys. Rev. D **80**, 085021 (2009).

[21]O. Kenneth and I. Klich, Phys. Rev. Lett. **97**, 160401 (2006).

[22]C. P. Bachas, J. Phys. A **40**, 9089 (2007).

[23]S. J. Rahi, M. Kardar, and T. Emig, Phys. Rev. Lett. **105**, 070404 (2010).

[24]A. Forrow and N. Graham, Phys. Rev. A **86**, 062715 (2012).

[25]E. Buks and M. L. Roukes, Phys. Rev. B **63**, 033402 (2001).

[26]F. Capasso, J. N. Munday, D. Iannuzzi, and H. B. Chan, IEEE J. Quantum Electron. **13**, 400 (2007).

[27]J. N. Munday and F. Capasso, Int. J. Mod. Phys. A **25**, 2252 (2010).

[28]G. L. Klimchitskaya, U. Mohideen, and V. M. Mostepanenko, Rev. Mod. Phys. **81**, 1827 (2009).

[29]R. Zhao et al., Science **364**, 984 (2019).

[30]B. Munkhbat, A. Canales, B. Küçüköz, D. G. Baranov, and T. O. Shegai, Nature **597**, 214 (2021).

[31]M. Levin, A. P. McCauley, A. W. Rodriguez, M. T. Homer Reid, and S. G. Johnson, Phys. Rev. Lett. **105**, 090403 (2010).

[32]P. P. Abrantes, Y. França, F.S.S. Rosa, C. Farina, and R. M. Souza, Phys. Rev. A **98**, 012511 (2018).

[33]Q. D. Jiang and F. Wilczek, Phys. Rev. B **99**, 125403 (2019).

[34]F. Schmidt, A. Callegari, A. Daddi-Moussa-Ider, B. Munkhbat, R. Verre, T. Shegai, M. Käll, H. Löwen, A. Gambassi, and G. Volpe, `https://doi.org/10.48550/arXiv.2202.10926` (2022).

[35]M. E. Fisher and P. G. de Gennes, C. R. Acad. Paris B **287**, 207 (1978).

[36]V. N. Marachevsky, Phys. Scr. **64**, 205 (2001).

[37]J. S. Høye, I. Brevik, and J. B. Aarseth, Phys. Rev. E **63**, 051101 (2001).

[38]I. Brevik, J. B. Aarseth, and J. S. Høye, Phys. Rev. E **66**, 026119 (2002).

[39]I. Brevik, E. K. Dahl, and G. O. Myhr, J. Phys. A Math. Gen. **38**, L49 (2005).

[40]D. A. R. Dalvit, F. C. Lombardo, F. D. Mazzitelli, and R. Onofrio, Phys. Rev. A **74**, 020101 (2006).

[41]V. N. Marachevsky, Phys. Rev. D **75**, 085019 (2007).

[42]M. Bordag and V. Nikolaev, J. Phys. A. **42**, 415203 (2009).

[43]S. Zaheer, S. J. Rahi, T. Emig, and R. L. Jaffe, Phys. Rev. A **82**, 052507 (2010).

[44]L. P. Teo, Phys. Rev. D **82**, 085009 (2010).

[45]S. J. Rahi and S. Zaheer, Phys. Rev. Lett. **104**, 070405 (2010).

[46]P. Parashar, K. A. Milton, K. V. Shajesh, and I. Brevik, Phys. Rev. D **96**, 085010 (2017).

[47]K. A. Milton, J. Phys. A Math. Gen. **37**, 6391 (2004).

[48]M. Bordag and D.V. Vassilevic, J. Phys. A Math. Gen. **32**, 8247 (1999).

[49]M. Bordag, K. Kirsten, and D. Vassilevich, Phys. Rev. D **59**, 085011 (1999).

[50]Y. N. Demkov and V. N. Ostrovskii, *Zero-Range Potentials and Their Applications in Atomic Physics* (Plenum Press, New York, 1988).

[51]M. Bordag and J. M. Munoz-Castaneda, Phys. Rev. D **91**, 065027 (2015).

[52]M. Bordag and I. G. Pirozhenko, Phys. Rev. D **95**, 056017 (2017).

[53]P. Kurasov, J. Math. Anal. Appl. **201**, 297 (1996).

[54]F.A.B. Coutinho, Y. Nogami, and J. F. Perez, J. Phys. A Math. Gen. **30**, 3937 (1997).

[55]S. Albeverio, F. Gesztesy, R. Høegh-Krohn, and H. Holden, *Solvable Models in Quantum Mechanics*, Second (AMS Chelsea Publishing, Providence, RI, 2005).

[56]L. J. Boya and E.C.G. Sudarshan, Int. J. Theor. Phys. **35**, 1063 (1996).

[57]D. J. Griffiths, J. Phys. A Math. Gen. **26**, 2265 (1993).

[58]F.A.B. Coutinho, Y. Nogami, and F. M. Toyama, Can. J. Phys. **90**, 383 (2012).

[59]M. Gadella, J. Negro, and L. M. Nieto, Phys. Lett. A **373**, 1310 (2009).

[60]S. Fassari, M. Gadella, L. Glasser, and L. Nieto, Ann. Phys. **389**, 48 (2018).

[61]M. Gadella, M. L. Glasser, and L. M. Nieto, Int. J. Theor. Phys. **50**, 2144 (2011).

[62]M. Gadella, M. L. Glasser, and L. M. Nieto, Int. J. Theor. Phys. **50**, 2191 (2011).

[63]J. M. Muñoz Castañeda and J. M. Mateos Guilarte, Phys. Rev. D **91**, 025028 (2015).

[64]M. Gadella, J. M. Guilarte, J. M. Muñoz-Castañeda, and L. M. Nieto, J. Phys. A **49**, 015204 (2016).

[65]M. Gadella, M. A. García-Ferrero, S. González-Martín, and F. H. Maldonado Villamizar, Int. J. Theor. Phys. **53**, 1614 (2014).

[66]J. J. Alvarez, M. Gadella, L. P. Lara, and F. H. Maldonado-Villamizar, Phys. Lett. A **377**, 2510 (2013).

[67]J. J. Alvarez, M. Gadella, and L. M. Nieto, Int. J. Theor. Phys. **50**, 2161 (2011).

[68]L. M. Nieto, M. Gadella, J. Mateos-Guilarte, J. M. Munoz-Castaneda, and C. Romaniega, "Some Recent Results on Contact or Point Supported Potentials", in *Geometric Methods in Physics XXXVIII* (Springer, 2020), pp. 197–219.

[69]M. Gadella, J. M. Guilarte, J. M. Muñoz-Castañeda, L. M. Nieto, and L. Santamaría-Sanz, Eur. Phys. J. Plus **135**, 1 (2020).

[70]J. S. Avery, J. Comput. App. Math. **233**, 1366 (2010).

[71]S. Albeverio and P. Kurasov, *Singular Perturbations of Differential Operators*, Vol. 271, London Mathematical Society: Lecture Notes Series (Cambridge University Press, 2000).

[72]T. R. Govindarajan and J. M. Munõz-Castañeda, Mod. Phys. Lett. A **31**, 1650210 (2016).

[73]M. Bordag, D. Vassilevich, H. Falomir, and E. M. Santangelo, Phys. Rev. D **64**, 045017 (2001).

[74]J. M. Muñoz-Castañeda, L. M. Nieto, and C. Romaniega, Ann. Phys. **400**, 246 (2019).

[75]V. Bargmann, Proc. Natl. Acad. Sci. **38**, 961 (1952).

[76]F. W. Olver, D. W. Lozier, R. F. Boisvert, and C. W. Clark, *NIST Handbook of Mathematical Functions* (Cambridge University Press, New York, 2010).

[77]A. Sharma, S. Gora, J. Bhagavathi, and O.S.K. S. Sastri, Am. J. Phys. **88**, 576 (2020).

[78]V. Mukhanov and S. Winitzki, *Introduction to Quantum Effects in Gravity* (Cambridge university press, 2007).

[79]S. Coleman, *Aspects of Symmetry: Selected Erice Lectures* (Cambridge University Press, Cambridge, 1988).

[80]K. A. Milton, *The Casimir Effect: Physical Manifestations of Zero-Point Energy* (World Scientific, Singapore, 2001).

[81]J. Dittrich, P. Exner, and P. Šeba, J. Math. Phys. **30**, 2875 (1989).

[82]M. Bordag and K. Kirsten, Phys. Rev. D **53**, 5753 (1996).

[83]M. Bordag, E. Elizalde, K. Kirsten, and S. Leseduarte, Phys. Rev. D **56**, 4896 (1997).

[84]K. Kirsten, *Spectral Functions in Mathematics and Physics* (Chapman & Hall/CRC, Boca Raton, FL, 2001).

[85]G. Fucci and K. Kirsten, J. Phys. A Math. Theor. **49**, 275203 (2016).

[86]J. R. Taylor, *Scattering Theory: The Quantum Theory of Nonrelativistic Collisions* (Dover Publications Inc., New York, 2006).

[87]M. Beauregard, M. Bordag, and K. Kirsten, J. Phys. A **48**, 095401 (2015).

[88]L. P. Teo, Int. J. Mod. Phys. A **27**, 1230021 (2012).

[89]V. V. Nesterenko and I. G. Pirozhenko, Phys. Rev. D **57**, 1284 (1998).

[90]J. R. Taylor, *Scattering Theory: The Quantum Theory of Nonrelativistic Collisions* (Dover Publications Inc., New York, 2006).

[91]G. W. Hanson and A. B. Yakovlev, *Operator Theory for Electromagnetics: an Introduction* (Springer Science & Business Media, 2013).

[92]B. R. Johnson, J. Opt. Soc. Am. A **16**, 845 (1999).

[93]B. Toni, *Advances in Interdisciplinary Mathematical Research: Applications to Engineering, Physical and Life Sciences*, Vol. 37, Chapter 3 (Springer Science & Business Media, 2014), p. 57.

[94]G. Barton, J. Phys. A Math. Gen. **37**, 1011 (2004).

[95]Y. Li, K. A. Milton, X. Guo, G. Kennedy, and S. A. Fulling, Phys. Rev. D **99**, 125004 (2019).

[96]F. Calogero, *Variable Phase Approach to Potential Scattering* (Academic, New York, 1967).

[97]B. R. Johnson, Appl. Opt. **27**, 4861 (1988).

[98]B. Sun, L. Bi, P. Yang, M. Kahnert, and G. Kattawar, *Invariant Imbedding T-matrix Method for Light Scattering by Nonspherical and Inhomogeneous Particles* (Elsevier, 2019).

[99]I. Cavero-Peláez, K. A. Milton, and K. Kirsten, J. Phys. A Math. Theor. **40**, 3607 (2007).

[100]I. Cavero-Peláez, J. M. Munoz-Castaneda, and C. Romaniega, Phys. Rev. D **103**, 045005 (2021).

[101]J. S. Høye, I. Brevik, J. B. Aarseth, and K. A. Milton, Phys. Rev. E **67**, 056116 (2003).

[102]C. Romaniega, M. Gadella, R. M. Id Betan, and L. M. Nieto, Eur. Phys. J. Plus **135**, 372 (2020).

[103]A. Martín-Mozo, L. M. Nieto, and C. Romaniega, Eur. Phys. J. Plus **137**, 1 (2022).

[104]C. Romaniega, Eur. Phys. J. Plus **136**, 327 (2021).

[105]C. Romaniega, Eur. Phys. J. Plus **136**, 1051 (2021).

[106]C. Romaniega, I. Cavero-Peláez, and J. M. Muñoz-Castañeda, "Casimir self-energy of a δ-δ' sphere", pending of acceptance (2022).

Part I

Study of spherical δ-δ' interactions

Chapter 1

Hyperspherical δ-δ' potentials

This chapter is adapted from:

Hyperspherical δ-δ' potentials

J. M. Muñoz-Castañeda[1], L. M. Nieto[1,2], C. Romaniega[1]

Annal of Physics **400**, 246 (2019)

DOI: https://doi.org/10.1016/j.aop.2018.11.017

[1]Departamento de Física Teórica, Atómica y Óptica, Universidad de Valladolid, 47011 Valladolid, Spain.

[2]IMUVA- Instituto de Matematicas, Universidad de Valladolid, 47011 Valladolid, Spain.

In this first chapter the spherical δ-δ' interaction for a d-dimensional space is defined. The bound states, scattering states and zero-energy states are computed. As stated above, these results will play a central role in the second part of this thesis.

1.1 Abstract

The spherically symmetric potential $a\,\delta(r-r_0)+b\,\delta'(r-r_0)$ is generalized for the d-dimensional space as a characterization of a unique self-adjoint extension of the free Hamiltonian. For this extension of the Dirac delta, the spectrum of negative, zero and positive energy states is studied in $d \geq 2$, providing numerical results for the expectation value of the radius as a function of the free parameters of the potential. Remarkably, only if $d = 2$ the δ-δ' potential for arbitrary $a > 0$ admits a bound state with zero angular momentum.

Chapter 2

Regular and δ-δ' potentials I

This chapter is adapted from:

An approximation to the Woods–Saxon potential based on a contact interaction

C. Romaniega[1], M. Gadella[1], R. M. Id Betan[2,3,4] and L. M. Nieto[1]

The European Physical Journal Plus **135**, 372 (2020)

DOI: https://doi.org/10.1140/epjp/s13360-020-00388-7

[1]Departamento de Física Teórica, Atómica y Óptica and IMUVA, Universidad de Valladolid, 47011. Valladolid, Spain.

[2]Instituto de Física Rosario (CONICET-UNR), Bv. 27 de Febrero 210 bis, S2000EZP Rosario, Argentina.

[3]Facultad de Ciencias Exactas, Ingeniería y Agrimensura (UNR), Av. Pellegrini 250, S2000BTP Rosario, Argentina.

[4]Instituto de Estudios Nucleares y Radiaciones Ionizantes (UNR), Riobamba y Berutti, S2000EKA Rosario, Argentina.

We now add a spherical well to the potential, extending the study of the singular interaction defined in the previous chapter using von Neumann's theory. We show how we can adapt the one-dimensional work to our system with singular and regular spherical potentials. We also characterize and calculate the number of bound states, extend some properties of continuous spherically symmetric potentials and describe the unstable quantum states. We indicate the possible use of the interaction as a first approximation of real physical systems, particularly for describing neutron energy levels for double magic nuclei.

2.1 Abstract

We study a nonrelativistic particle subject to a three-dimensional spherical potential consisting of a finite well and a radial δ-δ' contact interaction at the well edge. This contact potential is defined by appropriate matching conditions for the radial functions, thereby fixing a self-adjoint extension of the nonsingular Hamiltonian. Since this model admits exact solutions for the wave function, we are able to characterize and calculate the number of bound states. We also extend some well known properties of certain spherically symmetric potentials and describe the resonances, defined as unstable quantum states. Based on the Woods-Saxon potential, this configuration is implemented as a first approximation for a mean-field nuclear model. The results derived are tested with experimental and numerical data in the double magic nuclei ^{132}Sn and ^{208}Pb with an extra neutron.

Chapter 3

Regular and δ-δ' potentials II

This chapter is adapted from:

A solvable contact potential based on a nuclear model

A. Martín-Mozo, L. M. Nieto and C. Romaniega
The European Physical Journal Plus **137**, 33 (2022)

DOI: https://doi.org/10.1140/epjp/s13360-021-02247-5

Departamento de Física Teórica, Atómica y Óptica and IMUVA, Universidad de Valladolid, 47011. Valladolid, Spain.

In this chapter we continue the analysis of the previous one. We now add the static Coulomb potential of a uniformly charged sphere. This enables the study of proton energy states and, as in the previous paper, some applications for describing physical systems are indicated. These are based on the properties of confluent hypergeometric functions with complex arguments. In addition, we now find the optimal δ' contribution which best fits the available data for the nucleon level schemes of the nuclei ^{208}Pb, ^{40}Ca and ^{16}O.

3.1 Abstract

We extend previous work on the study of a particle subject to a three-dimensional spherical singular potential including a δ-δ' contact interaction. In this case, to have a more realistic model, we add a Coulombic term to a finite well and a radial δ-δ' contact interaction just at the edge of the well, which is where the surface of the nucleus would be. We first prove that we are able to define the contact potential by matching conditions for the radial function, fixing a self-adjoint extension of the nonsingular Hamiltonian. With these matching conditions, we are able to find analytic solutions of the wave function and focus the analysis on the bound state structure characterizing and computing the number of bound states. For this approximation for a mean-field Woods-Saxon model, the Coulombic term enables us to complete the previous study for neutrons analyzing the proton energy levels in some doubly magic nuclei. In particular, we find the appropriate δ' contribution fitting the available data for the neutron- and proton-level schemes of the nuclei ^{208}Pb, ^{40}Ca and ^{16}O.

Part II

Casimir-Lifshitz energy and pressure in cavities

Chapter 4

Interaction energy between two concentric δ-δ' spheres

This chapter is adapted from:

Casimir energy for concentric δ-δ' spheres

I. Cavero-Peláez[1,2], J. M. Munoz-Castaneda[3], and C. Romaniega[3]

Physical Review D **103**, 045005 (2021)

DOI: https://doi.org/10.1103/PhysRevD.103.045005

[1]Centro Universitario de la Defensa, Zaragoza, 50019, Spain.

[2]Departamento de Física Teórica, Facultad de Ciencias, Universidad de Zaragoza, Zaragoza, 50009, Spain.

[3] Departamento de Física Teórica, Atómica y Óptica and IMUVA, Universidad de Valladolid, 47011. Valladolid, Spain.

We begin the second part studying the interaction energy of a massless scalar field in the presence of two concentric δ-δ' spheres. As indicated, some results from the previous part of the thesis are needed. In particular, we have computed the interaction energy for the values of the potential such that there are no bound states in the quantum mechanical sense. In addition, the components of the $\mathbb{T}$ operators appearing in the representation of the interaction Casimir energy in terms of functional determinants are completely determined using the scattering data computed in the first part of the thesis.

4.1 Abstract

We study the vacuum interaction of a scalar field and two concentric spheres defined by a singular potential on their surfaces. The potential is a linear combination of the Dirac δ and the δ' interaction. The presence of the δ' term in the potential causes that it behaves differently when it is seen from the inside or from the outside of the sphere. We study different cases for positive and negative values of the delta prime coupling, keeping positive the coupling of the delta. As a consequence, we find regions in the space of couplings, where the energy is positive, negative or zero. Moreover, the sign of the δ' couplings causes different behavior on the value of the Casimir energy for different values of the radii. This potential gives rise to general boundary conditions with limiting cases defining Dirichlet and Robin boundary conditions that allows us to simulate purely electric or purely magnetic spheres.

Chapter 5

Self-energy of a δ-δ' sphere

This chapter is adapted from:

Casimir self-energy of a δ-δ' sphere

C. Romaniega[1], J. M. Munoz-Castaneda[1], and I. Cavero-Peláez[2,3]

[1] Departamento de Física Teórica, Atómica y Óptica and IMUVA, Universidad de Valladolid, 47011. Valladolid, Spain.

[2]Centro Universitario de la Defensa, Zaragoza, 50019, Spain.

[3]Departamento de Física Teórica, Facultad de Ciencias, Universidad de Zaragoza, Zaragoza, 50009, Spain.

We continue the analysis of the previous chapter computing the self-energy contribution to the pressure on a δ-δ' sphere using the zeta function regularization method. In this context, the energy is completely determined by the Jost function for each value of the angular momentum, which is easily found with the scattering phase shifts of the first part of the thesis. We find a simple relation between the couplings of the δ and δ' interactions such that the Casimir self-energy is unambiguously defined, computing the relevant heat kernel coefficient. We also check our results against particular cases previously studied in the literature.

5.1 Abstract

We extend previous work on the vacuum energy of a massless scalar field in the presence of singular potentials. We consider a single sphere defined by the so-called δ-δ' interaction. Contrary to the Dirac δ potential, we find a nontrivial one-parameter family of potentials such that the regularization procedure gives an unambiguous result for the Casimir self-energy. The procedure employed is based on the zeta function regularization and the cancellation of the heat kernel coefficient a_2. The results obtained are in agreement with particular cases, such as the Dirac δ or Robin and Dirichlet boundary conditions.

5.2 Introduction

Quantum vacuum fluctuations are known to give rise to forces between two distinct bodies as well as pressure on the surface of a single object. This macroscopic manifestation of the vacuum state associated to quantum fields has been investigated and measured in some special cases, achieving a level of concordance between theory and experiments that has astonished the community (see Refs. [1, 2] for general reviews).

From a quantum field theoretical point of view, the zero-point energy due to the quantum vacuum fluctuations carries divergences. The appearance of the Casimir energy has stressed the importance of dealing with divergences and acquiring a deep understanding of their nature to the point of extracting the finite part of the zero-point fluctuations, isolating the different divergent contributions and obtaining a physically meaningful result. After regularization and renormalization, the part of the quantum vacuum energy that encloses the quantum vacuum interaction between two objects is unambiguous and leads to a finite force between the bodies [1, 3–5]. However, in general, the self-energy of a single object is only unambiguously defined for the case of massive quantum vacuum fluctuations. In the case of massless quantum fields, the self-energy is only defined in a unique way for a few cases involving special geometries and boundary conditions. For example, it is well known that in the dilute case the Casimir energy, that can also be calculated as the sum of the van der Waals interactions, is unambiguously identified once the surface and volume divergences are removed [6–8]. Perfectly conducting as well as dielectric geometries such as spheres or cylinders have been computed resulting on finite answers for the Casimir stress on the surface [9–12]

In all the cases mentioned above, different techniques for regularizing the vacuum self-stress and extracting the divergences have been used. From the zeta function regularization, to point splitting, analytic continuation or the calculation of heat kernel coefficients, several methods are used to understand the meaning and nature of the infinities arising from summing the zero-point frequencies. The difficulties that the study of the self-energies carries have been discussed broadly and Bordag et al. were the first ones discussing these divergences by computing the heat kernel coefficients [13]. Furthermore, Bordag, Kirsten, Vassilevich, and others, have given analytic formulas that enable the characterization of the infinities and the ambiguities appearing in the calculation of quantum vacuum self-energies in terms of the heat kernel coefficients [14, 15].

In a recent paper [16] (Chapter 4 of this thesis), we calculated the interaction energy between two concentric spherical shells mimicked by δ-δ' singular potentials on the surfaces. In this case the Casimir energy can be written as

$$E_{\mathrm{C}} = E_1 + E_2 + E_{\mathrm{int}}, \tag{5.1}$$

being E_{int} the interaction energy, which can be determined unambiguously, and E_1 and E_2 the self-energies of the first and second body, respectively. Since the divergent contributions depend on the characteristics of the body, like the radius of the sphere, a renormalization procedure is in general needed for the self-energies in order to give a meaningful result. When the spheres (or any other geometrical body) are one outside the other, the force between the bodies can be obtained as the derivative of the energy with respect to the distance between the objects. Although a similar analysis can be performed for a sphere inside a cavity [17], for two concentric spheres the interaction energy has no independent meaning and to obtain a full understanding we need to know the self-energy. Indeed, in this configuration the total interaction force acting on the spheres vanishes, although the pressure acting on their surfaces does not. This pressure is now defined as the derivative with respect to the radius of the shell, and the self-energy also depends on it.

In this paper we focus on the pressure on a single sphere, thus extending the work of our previous aforementioned paper [16]. In the latter, we studied the sign of the interaction energy for a massless scalar field in the presence of two concentric δ-δ' spheres employing the TGTG representation of the energy. The same representation

was used in [18] (Chapter 6 of this thesis), where the pressure acting on a dielectric sphere enclosed within a magnetodielectric cavity was studied. Although the sign of the interaction pressure was determined for quite general inhomogeneous permittivities and permeabilities, the self-pressure of the sphere was only well defined in the known dilute limit [13]. Indeed, as we have stated, there are a few cases in which the self-energy has an unambiguous meaning [19]. One is the aforementioned dilute limit [12, 13], a magnetodielectric object when the speed of light is the same inside and outside [20, 21] or a perfectly conducting spherical or cylindrical shell [9, 10]. For a massless scalar field, an unambiguously finite result is found up to second order for the δ potential weak limit [22], as well as for for Dirichlet and Neumann boundary conditions. For these boundary conditions a cancellation of the divergences occurs when the whole space is considered [1]. However, for Robin boundary conditions this is no longer the case, and the cancellation only occurs for certain values of the parameter [14].

In this paper we will employ the zeta function regularization for analyzing the divergences. Within this approach, the energy is expressed in terms of the zeta function associated with a Schrödinger-type operator P

$$E_0(s) = \frac{\mu^{2s}}{2} \sum_n \omega_n^{1-2s} = \frac{\mu^{2s}}{2} \zeta_P(s - \frac{1}{2}), \tag{5.2}$$

where μ is a parameter with dimensions of mass introduced to keep the right dimensions and $\hbar = c = 1$. The zeta function associated with the operator determining the modes of the system is

$$\zeta_P(s) = \sum_n \lambda_n^{-s}, \qquad P\varphi_n(\boldsymbol{x}) = \lambda_n \varphi_n(\boldsymbol{x}). \tag{5.3}$$

In our case, we have $P = -\Delta + V_{\delta\text{-}\delta'}(r)$, where the potential represents the spherical singular interaction. From the asymptotic behaviour of the eigenvalues of this operator, indeed, for any second order elliptic differential operator [23], the sum (5.2) is divergent for $s = 0$ and it needs to be regularized. Once the divergences are identified, we need to renormalize the resulting expression. Bordag, Kirsten, Vassilevich and their collaborators demonstrated that the self-energy for massless scalar fields is defined in a unique way only if the heat kernel coefficient a_2 of the operator P given above is identically zero.

The aim of this paper is to study a complicated enough interaction to obtain nontrivial systems for which $a_2 = 0$, unlike what happens for the δ potential, and simple enough to proceed in an analytic way. The δ-δ' potential is chosen since it has two couplings that will enable, for certain particular cases, the cancellation of the a_2 heat kernel coefficient. This point interaction was introduced in [24] and studied in different contexts over the years [25–28], where many analytical results have been obtained.

The paper is organized as follows. In Section 5.3 we show previous results concerning the δ-δ' potential obtained in [29] (Chapter 1 of this thesis). In Section 5.4 we compute the quantum vacuum energy for a three-dimensional spherical shell mimicked by a radial δ-δ' potential using the zeta function regularization, and obtain those particular values for the couplings that give rise to a heat kernel coefficient a_2 identically zero. Section 5.5 shows the numerical results for the finite quantum vacuum self-energy and pressure when unambiguously defined. Finally, in Section 5.6 we present our conclusions and further comments. At the end, we include the Appendix where we present some particular cases that enable us to check our calculations by obtaining results already published by other authors.

5.3 δ-δ' potential on a spherical shell

Let us consider a single spherical shell defined by the singular potential

$$V_{\delta\text{-}\delta'}(r) = \lambda_0\delta(r-r_0) + 2\lambda_1\delta'(r-r_0), \quad r_0 \in \mathbb{R}^+. \tag{5.4}$$

The system of units chosen implies that $[\lambda_0] = L^{-1}$, and $[\lambda_1] = 1$. The scalar field satisfies the Klein-Gordon equation which, after taking its time Fourier transform, is

$$[-\Delta + V_{\delta\text{-}\delta'}(r)]\,\varphi(\mathbf{x}) = \omega^2\varphi(\mathbf{x}). \tag{5.5}$$

Due to the spherical symmetry of the system, the solutions can be written as

$$\varphi(\mathbf{x}) = \sum_{\ell=0}^{\infty}\sum_{m=-\ell}^{\ell}\rho_\ell(r)Y_{\ell m}(\theta,\phi), \tag{5.6}$$

where $Y_{\ell m}(\theta,\phi)$ are the spherical harmonics. The nonrelativistic Schrödinger Hamiltonian in Eq. (5.5) has been studied in detail in [29], where the potential $V_{\delta\text{-}\delta'}(r)$ is defined by matching conditions on the surface of the sphere with radius r_0 over the space of field modes as

$$\begin{pmatrix} \rho_\ell(r_0^+) \\ \rho'_\ell(r_0^+) \end{pmatrix} = \begin{pmatrix} \alpha & 0 \\ \widetilde{\beta} & \alpha^{-1} \end{pmatrix} \begin{pmatrix} \rho_\ell(r_0^-) \\ \rho'_\ell(r_0^-) \end{pmatrix}. \tag{5.7}$$

The prime here, and throughout the text, indicates derivative with respect to the argument and $r_0^\pm$ denotes the limit to r_0 taken from the right or from the left, respectively. We have also defined

$$\alpha := \frac{1+\lambda_1}{1-\lambda_1}, \qquad \widetilde{\beta} := \frac{\widetilde{\lambda}_0}{1-\lambda_1^2}, \qquad \widetilde{\lambda}_0 := -\frac{4\lambda_1}{r_0} + \lambda_0. \tag{5.8}$$

These matching conditions are ill defined if $\lambda_1 = \pm 1$. In these cases we can write [27]

$$\begin{aligned} &\rho_\ell(r_0^-) = 0, \quad \rho'_\ell(r_0^+) - D^+\rho_\ell(r_0^+) = 0 \quad \text{if} \quad \lambda_1 = +1, \\ &\rho_\ell(r_0^+) = 0, \quad \rho'_\ell(r_0^-) + D^-\rho_\ell(r_0^-) = 0 \quad \text{if} \quad \lambda_1 = -1, \end{aligned} \tag{5.9}$$

where $D^\pm = 4/(\lambda_0 \mp 4r_0^{-1})$. Notice that there is a typo in Eq. (30) in [16]. The eigenvalues are not known for this problem, so the explicit summation shown in (5.3) can not be performed. However, using Cauchy's formula, we can write the Casimir self-energy in terms of the Jost function $f_\ell(\kappa)$ as

$$E_0(s) = -\mu^{2s}\frac{\cos\pi s}{\pi}\sum_{\ell=0}^{\infty}\nu\int_0^\infty \mathrm{d}\kappa\,\kappa^{1-2s}\frac{\partial}{\partial\kappa}\log f_\ell(\kappa), \tag{5.10}$$

where the volume energy has already been subtracted [30]. For each value of the angular momentum this function satisfies [31]

$$\frac{f_\ell(\omega)}{f_\ell^*(\omega)} = e^{-2i\delta_\ell(\omega)}, \tag{5.11}$$

being $\delta_\ell(\omega)$ the scattering phase shift. For the potential in Eq. (5.4) we computed these phase shifts in [29] . From this we obtain

$$f_\ell(\kappa) = 1 + \frac{\lambda_0 r_0 - 2\lambda_1}{\lambda_1^2 + 1} I_\nu(y) K_\nu(y) - \frac{2\lambda_1 y}{\lambda_1^2 + 1} (I_\nu(y) K_\nu(y))', \tag{5.12}$$

where

$$\omega := i\kappa, \qquad \nu := \ell + \frac{1}{2}, \qquad y := \kappa r_0. \tag{5.13}$$

By turning off the coefficient of the δ' term in the potential, this expression reduces to the known result of the Jost function corresponding to a spherical shell with a δ potential on its surface [13],

$$f_\ell(\kappa) = 1 + r_0 \lambda_0 I_\nu(y) K_\nu(y). \tag{5.14}$$

5.4 Zeta function regularization

The zeta function is connected with the heat kernel $K(t)$ through the Mellin transform

$$\zeta(s) = \int_0^\infty \mathrm{d}t \, \frac{t^{s-1}}{\Gamma(s)} K(t), \tag{5.15}$$

where

$$K(t) = \sum_n e^{-\lambda_n t}. \tag{5.16}$$

At $s = 0$ this expression is exponentially decreasing for large t. The trouble comes when t is small. For that we use the asymptotic expansion [15]

$$K(t) \sim \frac{1}{(4\pi t)^{3/2}} \sum_n a_{n/2} t^{n/2}. \tag{5.17}$$

Taking these expressions into account and using the Casimir energy for massless scalar field as in Eq. (5.2), we find the result

$$E_0^{\mathrm{as}}(s) = -\frac{a_2}{32\pi^2} \left(\frac{1}{s} + 2\log(\mu r_0) \right) + E_0^{\mathrm{an}} + O(s), \tag{5.18}$$

where the superindex -as stands for asymptotic and -an for the analytic part. Contrary to massive fields, where the large-mass normalization condition ensures the absence of ambiguities, the only way to get a universal answer for our massless field is to consider configurations such that $a_2 = 0$. In this case, the log term containing the parameter μ, resulting from the regularization, disappears. In addition, with these cancellation no renormalization procedure is needed. Therefore, we look for those cases such that $a_2 = 0$, where a_2 can be identified as the coefficient of the divergent term in the vacuum energy. Specifically, this coefficient can be computed analyzing the behavior of the zeta function given in Eq. (5.2) if we take into account Eqs. (5.15) and (5.17). In particular,

$$a_n = \operatorname*{Res}_{s=\frac{3}{2}-n} \left((4\pi)^{\frac{3}{2}} \Gamma(s) \, \zeta(s) \right), \quad 2n \in \mathbb{N}_{\geq 0}. \tag{5.19}$$

Note that the self-energy given by Eq. (5.10) is not well defined for $s = 0$ due to the asymptotic behaviour of the integrand [14]. Therefore, we can extend the strip of

convergence in order to include $s = 0$ adding and then subtracting the appropriate asymptotic terms. In consequence, we define

$$E_0^{\text{fin}} := -\frac{1}{\pi}\sum_{\ell=0}^{\infty}\nu\int_0^{\infty}\mathrm{d}\kappa\,\kappa\frac{\partial}{\partial\kappa}\left(\log f_\ell(\kappa) - \log f_\ell^{\text{as}}(\kappa)\right), \tag{5.20}$$

as the finite part of the energy at $s = 0$ and

$$E_0^{\text{as}}(s) := -\mu^{2s}\frac{\cos\pi s}{\pi}\sum_{\ell=0}^{\infty}\nu\int_0^{\infty}\mathrm{d}\kappa\,\kappa^{1-2s}\frac{\partial}{\partial\kappa}\log f_\ell^{\text{as}}(\kappa), \tag{5.21}$$

the asymptotic one. Note that the definition of $\log f_\ell^{\text{as}}(\kappa)$ is determined by requiring E_0^{fin} to become finite. We achieve that by expanding the Jost function using its uniform asymptotic expansion [32] up to third order in $1/\nu$. This allows us to write the argument of the logarithm as

$$f_\ell^{\text{as}}(\kappa) \approx 1 + x(\nu),$$

where $x(\nu) \to 0$ when $\nu \to \infty$. Then, we expand the logarithm in Eq. (5.21) as a power series,

$$\log f_\ell^{\text{as}}(\kappa) := \sum_{n=1}^{N=3}\sum_{i=n}^{3n} C_{n,i}\frac{t^i(z)}{\nu^n}, \tag{5.22}$$

where $t(z) := 1/\sqrt{1+z^2}$ and $z = \kappa r_0/\nu$. Note that if we subtract N terms we move the strip of convergence $N/2$ to the left, so subtracting the first three is enough to isolate the analytic part of the zeta function [14]. Nonetheless, more terms could be subtracted for improving the numerical evaluation of E_0^{fin}. The first nonzero coefficients $C_{n,i}$ are

$$\begin{aligned}
C_{1,1} &= \frac{\lambda_0 r_0}{2(\lambda_1^2+1)},\ C_{1,3} = -\frac{\lambda_1}{\lambda_1^2+1},\\
C_{2,2} &= -\frac{\lambda_0^2 r_0^2}{8\left(\lambda_1^2+1\right)^2},\ C_{2,4} = \frac{\lambda_0\lambda_1 r_0}{2\left(\lambda_1^2+1\right)^2},\ C_{2,6} = -\frac{\lambda_1^2}{2\left(\lambda_1^2+1\right)^2},\\
C_{3,3} &= \frac{2\lambda_0^3 r_0^3 + 3\left(\lambda_1^2+1\right)^2\left(4\lambda_1+\lambda_0 r_0\right)}{48\left(\lambda_1^2+1\right)^3},\ C_{3,5} = -\frac{2\lambda_0^2\lambda_1 r_0^2 + 3\left(\lambda_1^2+1\right)^2\left(9\lambda_1+\lambda_0 r_0\right)}{8\left(\lambda_1^2+1\right)^3},\\
C_{3,7} &= \frac{120\lambda_1\left(\lambda_1^2+1\right)^2 + \lambda_0\left(5\lambda_1^4+18\lambda_1^2+5\right)r_0}{16\left(\lambda_1^2+1\right)^3},\ C_{3,9} = -\frac{\lambda_1\left(105\lambda_1^4+218\lambda_1^2+105\right)}{24\left(\lambda_1^2+1\right)^3}.
\end{aligned}$$

For $\lambda_1 = 0$, i.e., δ potential, we obtain the coefficients $X_{n,i}$ found in [33] and [13], although there is a minus sign missing in the coefficient $X_{2,2}$ in [13].

5.4.1 Heat kernel coefficient a_2

The purpose of this section is to analyze $E_0(s)$ as $s \to 0$ in order to discuss the divergences. Note that, by definition, E_0^{fin} gives no contribution to the poles at $s = 0$ so the divergences are only contained in $E_0^{\text{as}}(s)$. The integral to be computed in (5.21), after

performing the change of variables $z = \kappa r_0/\nu$, is

$$I = \frac{(r_0\mu)^{2s}}{r_0}\nu^{1-2s}\int_0^\infty \mathrm{d}z\, z^{1-2s}\frac{\partial}{\partial z}\log f_\ell^{\mathrm{as}}(z),$$

which can be easily solved using

$$\int_0^\infty \frac{z^n}{(z^2+1)^b}\,\mathrm{d}z = \frac{\Gamma\left(\frac{n+1}{2}\right)\Gamma\left(b-\frac{n}{2}-\frac{1}{2}\right)}{2\Gamma(b)}.$$

Now we perform the sum over ν in $E_0^{\mathrm{as}}(s)$. This can be written in terms of the Hurwitz zeta function for the three values of n

$$\sum_{\ell=0}^\infty \nu^{1-n+1-2s} = \sum_{\ell=0}^\infty \nu^{2-n-2s} = \zeta\left(n+2s-2,\frac{1}{2}\right).$$

The latter satisfies the following identity involving the Riemann zeta function

$$\zeta\left(n+2s-2,\frac{1}{2}\right) = (2^{2s+n-2}-1)\zeta(n+2s-2).$$

It is then clear that the contribution for $n = 2$ vanishes. Computing the residue we identify the a_2 coefficient of the singularity, finding

$$a_2 = \frac{2\pi\left(128\lambda_1^3+140\lambda_0^2\lambda_1 r_0^2-35\lambda_0^3 r_0^3-224\lambda_0\lambda_1^2 r_0\right)}{105\left(\lambda_1^2+1\right)^3 r_0}. \tag{5.23}$$

In addition, E_0^{an} in Eq. (5.18) is given by

$$\begin{aligned}E_0^{\mathrm{an}} = {}& \frac{1}{5040\pi r_0\left(\lambda_1^2+1\right)^3}\left(-64\lambda_1^3(12\gamma-1+36\log 2)-420\lambda_0^2\lambda_1 r_0^2(2\gamma-1+\log 64)\right.\\ &+210\lambda_0^3 r_0^3(\gamma-1+\log 8)-21\lambda_0 r_0\left(5\lambda_1^4(-12\log A+1+\log 8)\right.\\ &\left.\left.-2\lambda_1^2(60\log A-13+81\log 2)-60\log A+\gamma\left(5\lambda_1^4-54\lambda_1^2+5\right)+5+15\log 2\right)\right),\end{aligned}$$

where A is the Glaisher constant and γ is Euler's one. For $\lambda_1 = 0$, δ potential, we recover the results found in [13, 33]. From (5.23), we find that there is a family of parameters that make a_2 vanish and therefore defines the self-stress over the sphere without ambiguities. These couplings satisfy

$$\lambda_1 = \frac{1}{24}\left(\sqrt[3]{42\sqrt{30}+224}-\frac{14^{2/3}}{\sqrt[3]{3\sqrt{30}+16}}+14\right)\lambda_0 r_0.$$

There are other two combinations of the couplings such that $a_2 = 0$, but they involve complex solutions. Consequently, the self-energy is properly defined if

$$c_0\lambda_1 = \lambda_0 r_0, \qquad c_0 \simeq 1.20818671192. \tag{5.24}$$

5.5 Renormalized energy and pressure

Once $a_2 = 0$, the renormalized energy is unambiguously defined

$$E_0^{\text{ren}} := E_0^{\text{fin}} + E_0^{\text{an}}.$$

In contrast to E_0^{fin} and E_0^{an}, this quantity is uniquely defined since it does not depend on the number of terms subtracted. As we have stated, the renormalization is completely determined if the heat kernel coefficient $a_2 = 0$ [1]. For the δ potential this is only possible for the trivial case $\lambda_0 = 0$ [13], although the weak limit can be computed until second order [22]. Studying the divergences using Green's functions it is shown that they come from the surface term only [34].

5.5.1 Pressure on the sphere

The pressure acting on the surface of the sphere can be obtained from E_0^{ren}. To define this pressure we make use of the principle of virtual work. For our spherically symmetric system [35, 36]

$$p_0^{\text{ren}} = -\frac{1}{4\pi r_0^2}\frac{\partial E_0^{\text{ren}}}{\partial r_0}. \tag{5.25}$$

For the case in Eq. (5.24), where the self-energy is well defined, the finite and analytic parts of the renormalized energy become

$$E_0^{\text{fin}} = \frac{1}{\pi r_0}\sum_{\ell=0}^{\infty}\nu^2\int_0^{\infty}\mathrm{d}z\,(\log f_\ell(z) - \log f_\ell^{\text{as}}(z)) \tag{5.26}$$

and

$$E_0^{\text{an}} = \frac{F(\lambda_1, c_0)}{5040\pi\left(\lambda_1^2+1\right)^3 r_0}, \tag{5.27}$$

where we have integrated by parts in the first expression and the function $F(\lambda_1, c_0)$ is obtained from Eq. (5.23) setting $\lambda_0 r_0 = \lambda_1 c_0$. Both terms have the same dependence on r_0 and therefore,

$$\operatorname{sgn} p_0^{\text{ren}} = \operatorname{sgn} E_0^{\text{ren}}. \tag{5.28}$$

Indeed, E_0^{ren} can be written as $E_0^{\text{ren}} = e_0^{\text{ren}}/r_0$, being e_0^{ren} a numerical constant independent of r_0. Then,

$$E_0^{\text{ren}} = \frac{e_0^{\text{ren}}}{r_0}, \qquad p = \frac{e_0^{\text{ren}}}{4\pi r_0^4}. \tag{5.29}$$

5.5.2 Numerical evaluation

Now we compute E_0^{ren} when $a_2 = 0$. The finite part of the energy (5.26) can be calculated only numerically and for that we use a code in the interpreted programming language Python.

First, note that if (5.24) holds there are no bound states in the quantum mechanical sense. That is to say, with our potential in (5.5) we can not have $\omega^2 < 0$. For the latter we should change the integration contour in order to avoid the poles along the imaginary axis [31]. The absence of bound states can be proved with Proposition 2 in [29]. This result states that the quantum mechanical system admits bound states with

angular momentum from 0 to $\ell_{\max}$, being

$$\ell_{\max} = \left\lfloor -\frac{1}{2} + \frac{\lambda_1 - \frac{\lambda_0 r_0}{2}}{\lambda_1^2 + 1} \right\rfloor . \tag{5.30}$$

For the δ potential case we see that there are no bound states unless the potential is deep enough, $\lambda_0 r_0 < -1$, as expected. For the δ-δ' potential however, and under the condition in (5.24), there exist no bound states regardless of the value of λ_0. This can be easily proved noting that in this case

$$\ell_{\max} = -\frac{1}{2}\left\lfloor 1 + (2 - c_0)\frac{\lambda_1}{\lambda_1^2 + 1} \right\rfloor , \qquad \lambda_1 = \frac{\lambda_0 r_0}{c_0}, \tag{5.31}$$

which is always negative since $c_0 \in (0, 2)$. Indeed, this is clear if $\lambda_1 \leq 0$. If $\lambda_1 > 0$ we have $\lambda_1 / \left(\lambda_1^2 + 1\right) \leq 1/2$. Note that for $\lambda_1 = 1/2$, where $\ell_{\max} = 0$ there is no zero-mode either, see Sec. 4.2 of [29]. In addition, from [29] we know that bound states for positive values of λ_0 are only possible for two spatial dimensions.

We plot the renormalized vacuum energy as a function of λ_1 in Fig. 5.1. Note that only positive values are obtained, i.e., self-repulsion which tends to expand the sphere. A similar behaviour for the energy was found for the interaction energy be-

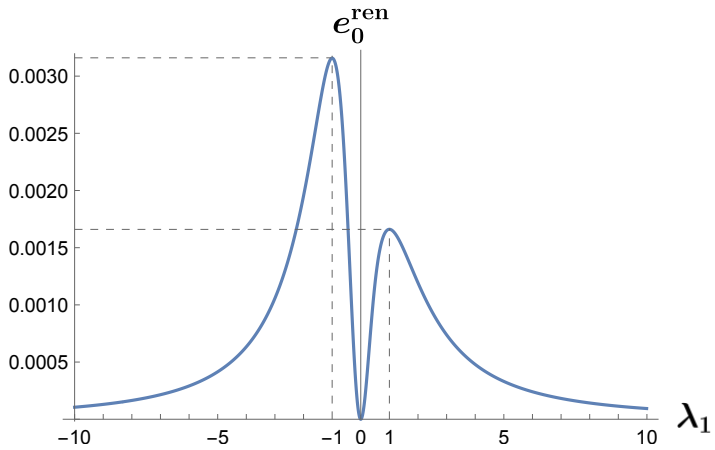

Figure 5.1: Renormalized energy for $r_0 = 1$, $E_0^{\text{ren}} = e_0^{\text{ren}}$, and $a_2 = 0$, i.e., $c_0\lambda_1 = \lambda_0$.

tween two concentric δ-δ' spheres [16]. For instance, the result is not symmetric under the change $\lambda_1 \to -\lambda_1$, contrary to what happens with δ-δ' plates [26]. In addition, the maximum values of the energy are found when we approach $\lambda_1 = \pm 1$ corresponding to Dirichlet and Robin boundary conditions, see Eq. (5.9). In particular, we have

$$\rho_\ell(r_0^-) = 0, \quad \rho_\ell'(r_0^+) + \frac{4r_0}{4 - c_0}\rho_\ell(r_0^+) = 0 \quad \text{if} \quad \lambda_1 = +1,$$
$$\rho_\ell(r_0^+) = 0, \quad \rho_\ell'(r_0^-) + \frac{4r_0}{4 + c_0}\rho_\ell(r_0^-) = 0 \quad \text{if} \quad \lambda_1 = -1.$$

Consequently, we have found a system, which is combination of Dirichlet and Robin boundary conditions inside and outside the sphere, whose renormalized self-energy is well defined. Notice that this is not trivial since for Dirichlet or Neumann boundary conditions $a_2 \neq 0$ if we only consider the interior or exterior region [1]. However, due to the dependence on odd powers of the extrinsic curvature, when the interior and exterior of the sphere are considered together, the divergences cancel each other.

For Robin boundary conditions even powers are also present, and the cancellation only occurs for special values of the Robin parameter [14]. Furthermore, the value of the self-energy and the self-pressure are of the same order of magnitude that the one found for Dirichlet boundary conditions, where $E_0^{\text{ren}} \simeq 0.0028168/r_0$. However, the results presented here are significantly lower than the one found for Neumann boundary conditions, where $E_0^{\text{ren}} \simeq -0.2238216/r_0$.

Note also that in the limit $\lambda_1 \to \pm\infty$ the self-energy goes to zero. This is in agreement with previous results [37] (Chapter 2 of this thesis) since this case corresponds to the configuration with no potential. These can be seen from Eq. (5.7), where the fields and their derivatives become continuous at the boundary when $\lambda_1 \to \pm\infty$. In the Appendix, we include two other consistency checks of our calculation. In particular, we have obtained the weak limit formula first computed in [22] for a Dirac δ spherical shell, and reproduced the numerical results in [38] for a spherical shell when approaching the decoupled limits $\lambda_1 \to \pm 1$.

5.6 Conclusions

In this paper we have added another example to the short list of simple configurations in which the Casimir self-energy for a massless field is unambiguously defined. This occurs due to a particular cancellation between the Dirac δ and the δ' interaction, Eq. (5.24). A similar cancellation arises when considering the Dirac δ and other type of singular interaction[1] defined by imposing matching conditions such that the derivative is continuous and there is a finite discontinuity in the radial function [39].

For the one-parameter family of values in which the energy and pressure are well defined, we only find positive values of both quantities. This leads to self-repulsion which tends to expand the sphere. The first example of self-repulsion was found by Boyer [9], refuting Casimir's model for the electron.

In the Appendix we have tested our results against the Dirac δ weak limit and Robin-Dirchlet boundary conditions. It is worth mentioning that our values of energy and pressure are similar to the ones obtained for a Dirichlet sphere. In addition, from this approach we see that we do not need to consider the interior and the exterior in an independent way. This is clear for matching conditions, but we also obtain this in the limit when we approach boundary conditions, even though a Jost function only perceives the exterior region for any opaque potential.

We observe some similarities between the self-energy and the interaction energy for concentric δ-δ' spheres [16] and a complete study of the total pressure will be performed in a forthcoming publication.

Acknowledgments

C.R. is grateful to G. Fucci for fruitful discussions at East Carolina University. C.R. thanks the Spanish Government for funding under the FPU-fellowships program FPU17/01475 and the FPU mobility program EST21/00286. C.R. acknowledges the support of the grant PID2020-113406GB-I0 funded by the MCIN (Spanish Government). I.C.P. would like to thank the support received from the grants PGC2018-095328-B-I00 funded by the *Agencia Estatal de Investigación* (Spanish Government) and the FEDER fund (EU), and 225351 funded by the DGA.

[1] This is the δ' interaction defined by Eq. (4) in the Introduction.

Appendix

As a consistency check, we compare our results with previous work. This can be done for particular values of $\{\lambda_0,\ \lambda_1\}$ where our potential simplifies to well known cases.

First, we assume $\lambda_1 = 0$ and small values of the δ coupling, i.e., the weak limit for the δ potential. In [22] it is proved that, expanding the log in the total energy, an unambiguously finite energy is obtained in second order of the coupling:

$$E_0^{(2)} = \frac{r_0}{32\pi}\lambda_0^2. \tag{5.32}$$

Our results are plotted in Fig. 5.2. Note that the third order term of the expansion is unambiguously divergent. Indeed, this was first proved in [13] and can be seen from our expressions. Specifically, from (5.18) we know that the divergence is proportional to a_2. For the δ potential we have already mentioned that $a_2 \neq 0$ except for the trivial case. In fact, a_2 is proportional to λ_0^3 as we can see from (5.23). In particular, the third

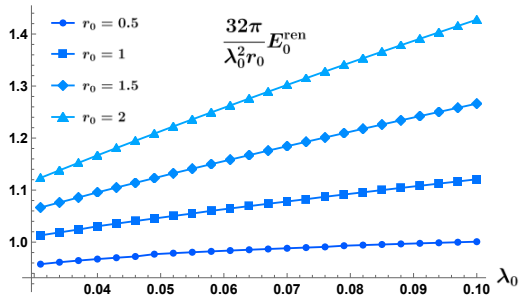

(a) $E_0^{\rm ren}$ multiplied by the inverse of $E_0^{(2)}$. Values close to one are expected when the approximation is fair enough.

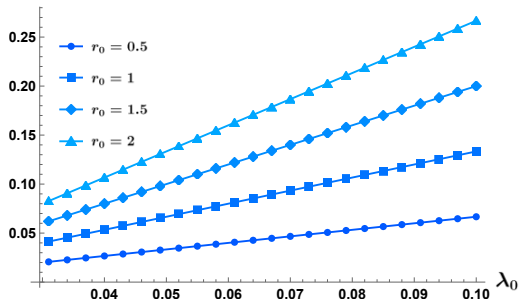

(b) The ratio $E_0^{(3)}/(E_0^{(2)}\zeta(1))$ is evaluated in order to check the relevance of each term.

Figure 5.2: Weak limit for the δ potential, $\lambda_1 = 0$ and small λ_0. Note that both $E_0^{(2)}$ and $E_0^{(3)}$ are positive quantities.

order term is [22]

$$E_0^{(3)} = \frac{r_0^2}{24\pi}\lambda_0^3\zeta(1). \tag{5.33}$$

Although the integral is convergent, the sum over the angular momentum is divergent. This is why the Riemann zeta function $\zeta(z)$ is evaluated at $z = 1$. In Fig. 5.2 we can see that the result is in good agreement for small values of λ_0. When the third order term becomes relevant the difference between $E_0^{(2)}$ and $E_0^{\rm ren}$ grows larger. Note that in our case the sum is computed until certain $\ell_{\rm max}$. In consequence $\zeta(1)$ is only evaluated up to that $\ell_{\rm max}$.

We can also verify the case $\lambda_1 \to \pm 1$ and $\lambda_0 = 0$ making use of known results for the electromagnetic field. In this case we approach the boundary conditions satisfied by the transverse electric (TE) mode and the transverse magnetic (TM) mode of the electromagnetic field in the presence of a perfectly conducting spherical shell [38]. Note that now we do not have the $\ell = 0$ contribution. In particular, in [38] it is found that for the TE mode plus $\ell = 0$, TE^0, the *renormalized* term of the zeta function inside and outside the sphere, $2e_0^{\rm ren}$, is

$$2e_0^{\rm ren}(\mathrm{TE}^0_{\rm in}) \simeq 0.00889, \quad 2e_0^{\rm ren}(\mathrm{TE}^0_{\rm out}) \simeq -0.00326.$$

For the TM mode plus $\ell = 0$, TM^0, this term inside and outside is

$$2e_0^{\mathrm{ren}}(\mathrm{TM}_{\mathrm{in}}^0) \simeq 0.02805, \quad 2e_0^{\mathrm{ren}}(\mathrm{TM}_{\mathrm{out}}^0) \simeq -0.07223.$$

For each mode we have a scalar problem satisfying Dirichlet (TE^0) or Robin (TM^0) boundary conditions. For the latter, the Robin boundary conditions are the ones in Eq. (5.9) with $\lambda_0 = 0$. Consequently, in a system with Robin inside and Dirichlet outside the renormalized energy should be

$$e_0^{\mathrm{ren}} \simeq \frac{0.02805 - 0.00326}{2} \simeq 0.012395.$$

With Dirichlet inside and Robin outside

$$e_0^{\mathrm{ren}} \simeq \frac{0.00889 - 0.07223}{2} \simeq -0.03167.$$

Bearing in mind Eq. (5.9), the previous systems can be reached with our potential setting $\lambda_0 = 0$ and $\lambda_1 \to \mp 1$, respectively. From our code we obtain

$$\begin{aligned} \lambda_0 = 0,\ \lambda_1 \to -1, \qquad & e_0^{\mathrm{ren}} \simeq \ \ 0.01241, \\ \lambda_0 = 0,\ \lambda_1 \to +1, \qquad & e_0^{\mathrm{ren}} \simeq -0.03166. \end{aligned}$$

We want to point out that in these cases $a_2 \neq 0$ so the renormalized vacuum energy is not properly defined. Nevertheless, this part of the zeta function can be computed in order to check our findings.

References for Chapter 5

[1] M. Bordag, G. L. Klimchitskaya, U. Mohideen, and V. M. Mostepanenko, *Advances in the Casimir Effect* (Oxford University Press, Oxford, 2009).

[2] K. A. Milton, *The Casimir Effect: Physical Manifestations of Zero-Point Energy* (World Scientific, Singapore, 2001).

[3] O. Kenneth and I. Klich, Phys. Rev. Lett. **97**, 160401 (2006).

[4] O. Kenneth and I. Klich, Phys. Rev. B **78**, 014103 (2008).

[5] S. J. Rahi, T. Emig, N. Graham, R. L. Jaffe, and M. Kardar, Phys. Rev. D **80**, 085021 (2009).

[6] I. Brevik, V. N. Marachevsky, and K. A. Milton, Phys. Rev. Lett. **82**, 3948 (1999).

[7] G. Barton, J. Phys. A Math. Gen. **32**, 525 (1999).

[8] A. Romeo and K. A. Milton, Phys. Lett. B **621**, 309 (2005).

[9] T. H. Boyer, Phys. Rev. **174**, 1764 (1968).

[10] L. L. DeRaad Jr and K. A. Milton, Ann. Phys. **136**, 229 (1981).

[11] K. A. Milton and Y. Jack Ng, Phys. Rev. E **55**, 4207 (1997).

[12] I. Cavero-Pelaez and K. A Milton, Ann. Phys. **320**, 108 (2005).

[13] M. Bordag, K. Kirsten, and D. Vassilevich, Phys. Rev. D **59**, 085011 (1999).

[14] K. Kirsten, *Spectral Functions in Mathematics and Physics* (Chapman & Hall/CRC, Boca Raton, FL, 2001).

[15] D. V. Vassilevich, Phys. Rep. **388**, 279 (2003).

[16]I. Cavero-Peláez, J. M. Munoz-Castaneda, and C. Romaniega, Phys. Rev. D **103**, 045005 (2021).

[17]S. J. Rahi and S. Zaheer, Phys. Rev. Lett. **104**, 070405 (2010).

[18]C. Romaniega, Eur. Phys. J. Plus **136**, 327 (2021).

[19]I. Cavero-Peláez, K. A. Milton, and K. Kirsten, J. Phys. A Math. Theor. **40**, 3607 (2007).

[20]I. Klich, Phys. Rev. D **61**, 025004 (1999).

[21]K. A. Milton, A. V. Nesterenko, and V. V. Nesterenko, Phys. Rev. D **59**, 105009 (1999).

[22]K. A. Milton, J. Phys. A Math. Gen. **37**, 6391 (2004).

[23]H. Weyl, Math. Ann. **71**, 441 (1912).

[24]P. Kurasov, J. Math. Anal. Appl. **201**, 297 (1996).

[25]M. Gadella, J. Negro, and L. M. Nieto, Phys. Lett. A **373**, 1310 (2009).

[26]J. M. Muñoz Castañeda and J. M. Mateos Guilarte, Phys. Rev. D **91**, 025028 (2015).

[27]S. Albeverio and P. Kurasov, *Singular Perturbations of Differential Operators*, Vol. 271, London Mathematical Society: Lecture Notes Series (Cambridge University Press, 2000).

[28]A. Martín-Mozo, L. M. Nieto, and C. Romaniega, Eur. Phys. J. Plus **137**, 1 (2022).

[29]J. M. Muñoz-Castañeda, L. M. Nieto, and C. Romaniega, Ann. Phys. **400**, 246 (2019).

[30]M. Bordag and K. Kirsten, Phys. Rev. D **53**, 5753 (1996).

[31]J. R. Taylor, *Scattering Theory: The Quantum Theory of Nonrelativistic Collisions* (Dover Publications Inc., New York, 2006).

[32]F. W. Olver, D. W. Lozier, R. F. Boisvert, and C. W. Clark, *NIST Handbook of Mathematical Functions* (Cambridge University Press, New York, 2010).

[33]M. Bordag and D.V. Vassilevic, J. Phys. A Math. Gen. **32**, 8247 (1999).

[34]I. Cavero-Peláez, K. A. Milton, and J. Wagner, Phys. Rev. D **73**, 085004 (2006).

[35]G. Barton, J. Phys. A Math. Gen. **37**, 1011 (2004).

[36]Y. Li, K. A. Milton, X. Guo, G. Kennedy, and S. A. Fulling, Phys. Rev. D **99**, 125004 (2019).

[37]C. Romaniega, M. Gadella, R. M. Id Betan, and L. M. Nieto, Eur. Phys. J. Plus **135**, 372 (2020).

[38]S. Leseduarte and A. Romeo, Ann. Phys. **250**, 448 (1996).

[39]K. A. Milton, J. Phys. A Math. Gen. **37**, R209 (2004).

Chapter 6

Casimir-Lifshitz pressure in cavities I

This chapter is adapted from:

Repulsive Casimir–Lifshitz pressure in closed cavities

C. Romaniega

The European Physical Journal Plus **136**, 327 (2021)

DOI: https://doi.org/10.1140/epjp/s13360-021-01308-z

Departamento de Física Teórica, Atómica y Óptica and IMUVA, Universidad de Valladolid, 47011. Valladolid, Spain.

In these two final chapters we study the interaction term of the energy for the electromagnetic field in the presence of more realistic bodies. Specifically, in this chapter we consider a dielectric sphere enclosed within an arbitrarily shaped magnetodielectric cavity. We determine, under general hypotheses, the sign of the interaction energy and pressure acting on the sphere. This is achieved by rewriting the expression in terms of functional determinants and analyzing the properties of the classical T matrices. In this sense, this approach is similar to the one employed in previous theorems. In addition, in this chapter and in the following we also obtain the Dzyaloshinskii-Lifshitz-Pitaevskii result on the sign of the interaction force as a limiting case. For a dilute dielectric ball we also include the self-energy contribution, obtaining a total repulsive pressure.

6.1 Abstract

We consider the interaction pressure acting on the surface of a dielectric sphere enclosed within a magnetodielectric cavity. We determine the sign of this quantity regardless of the geometry of the cavity for systems at thermal equilibrium, extending the Dzyaloshinskii-Lifshitz-Pitaevskii result for homogeneous slabs. As in previous theorems regarding Casimir-Lifshitz forces, the result is based on the scattering formalism. In this case, the proof follows from the variable phase approach of electromagnetic scattering. With this, we present configurations in which both the interaction and the self-energy contribution to the pressure tend to expand the sphere.

Chapter 7

Casimir-Lifshitz pressure in cavities II

This chapter is adapted from:

Casimir-Lifshitz pressure on cavity walls

C. Romaniega

The European Physical Journal Plus **136**, 1051 (2021)

DOI: https://doi.org/10.1140/epjp/s13360-021-02059-7

Departamento de Física Teórica, Atómica y Óptica and IMUVA, Universidad de Valladolid, 47011. Valladolid, Spain.

We continue the analysis of the previous chapter, now considering a dielectric object with a spherical cavity in which another arbitrarily shaped magnetodielectric object is enclosed. Due to the components of the $\mathbb{T}$ operator entering in the TGTG representation, we need to introduce some novel results of classical electromagnetic scattering for configurations with the source and detector inside the cavity. The latter is based on the Lippmann-Schwinger equation and an invariant imbedding procedure. As in the previous chapter, the results on the energy and pressure are generalized to finite temperature systems at thermal equilibrium. We also check against particular examples found in the literature like conducting shells and homogeneous spherical dielectrics.

The structures of this chapter and the previous one are very similar. We have exploited the derivation of Chapter 6, introducing the corresponding modifications needed for the study of the new configuration and a slightly different notation for some intermediate steps.

7.1 Abstract

We extend our previous work on the electromagnetic Casimir-Lifshitz interaction between two bodies when one is contained within the other. We focus on the fluctuation-induced pressure acting on the cavity wall, which is assumed to be spherical. This pressure can be positive or negative depending on the response functions describing the bodies and the medium filling the cavity. However, we find that under general hypotheses, the sign is independent of the geometry of the configuration. This result is based on the representation of the Casimir-Lifshitz energy in terms of transition operators. In particular, we study the components of these operators related to inside scattering amplitudes, adapting the invariant imbedding procedure to this unfamiliar scattering setup. We find that our main result is in agreement with the Dzyaloshinskii-Lifshitz-Pitaevskii result, which is obtained as a limiting case.

Conclusions and further work

Although the main findings of this thesis are explained in detail in the Introduction, we summarize here the key points and how they relate to further work.

We have first extended one-dimensional results on δ-δ' singular interactions to hyperspherical systems in Chapter 1. We have properly defined the interaction by means of matching conditions using the theory of self-adjoint extensions. We have also studied the spectrum of the total Hamiltonian. The major advantage over one-dimensional systems is the application to real physical situations. We have proved it by comparing with actual data in the context of mean-field nuclear models. In addition, the analysis of the spectrum is also employed for investigating vacuum fluctuations in the presence of classical backgrounds. We have studied the Casimir energy, modeling the background with δ-δ' spheres. Obviously, this is an idealization since we are assuming bodies with zero thickness. However, the study of Chapters 2 and 3 can be used to consider more realistic bodies. For instance, following the lines of Chapter 2, we can add a spherical well for modeling a homogeneous body with a singular interaction at the surface and proceed in the same manner for computing the energy. Note that the scattering phase shifts needed can be easily obtained. Specifically, Proposition 4 of Chapter 1, which is based on the asymptotic expression of the wave function, holds for any potential with finite support. We can then straightforwardly compute the appropriate components of the $\mathbb{T}$ operators for the interaction energy and compute the Jost function for the self-energy, proceeding in the same manner as in Chapters 4 and 5, respectively. Particularly, for the self-energy we should take into account that if we only had V_0, the heat kernel coefficient a_2 would never vanish. This is why we can add the singular interaction at the edge. Indeed, for a smooth potential $V(\boldsymbol{x})$ the heat kernel coefficient a_2 associated with the operator $-\Delta + V(\boldsymbol{x})$ is determined by [1]

$$a_2 = \frac{1}{2}\int_{\mathbb{R}^3} \mathrm{d}\boldsymbol{x}\, V(\boldsymbol{x})^2.$$

First, note that $V(\boldsymbol{x})^2$ has no meaning for our singular interaction. In addition, for this kind of potentials $a_2 = 0$ occurs if and only if we are in the free case, in which the Casimir energy vanishes. However, when boundary or matching conditions are present we can have nontrivial configurations in which $a_2 = 0$, as we have proved in Chapter 5. This is one of the reasons why there are not many configurations for massless scalar fields with an unambiguous self-energy [2].

Studying vacuum fluctuations from different fields can also yield many insights into the theoretical problems considered in this thesis. In this way, we are currently investigating the self-energy of a singular shell for a massive spinor field with spin one-half. This project started during my research stay at the department of Mathematics of East Carolina University (ECU) with Dr. Guglielmo Fucci at the beginning of 2022 [3]. For the Dirac operator the analogue of the δ-δ' interaction was first introduced by J. Dittrich, P. Exner and P. Šeba [4]. The approach is similar to the one described in [5] and a four-parameter family of matching conditions is found using the self-adjoint extension theory. However, in this case the analysis is more involved.

Specifically, the eigenvalue equation resulting from the free Dirac equation for a massive spinor field can be written as

$$H_0\varphi = E\varphi, \quad H_0 \equiv -i\alpha_i\partial_i + m\beta, \tag{7.1}$$

where $\psi(x)$ is a four-component bispinor and α_i and β define the suitable gamma matrices γ_μ. For the Dirac operator the conditions defining the spherical singular interaction at $r = R$ are given by

$$D\begin{pmatrix} f(R_+) \\ g(R_+) \end{pmatrix} + C\begin{pmatrix} f(R_-) \\ g(R_-) \end{pmatrix} = \begin{pmatrix} 0 \\ 0 \end{pmatrix}, \; \varphi(\vec{r}) = \frac{1}{r}\begin{pmatrix} if(r)\mathcal{Y}^{\sigma}_{\ell M}(\theta,\phi) \\ g(r)\sigma_r\mathcal{Y}^{\sigma}_{\ell M}(\theta,\phi) \end{pmatrix}, \tag{7.2}$$

where $\mathcal{Y}^{\sigma}_{\ell M}(\theta,\phi)$ are spherical spinors and C and D are real matrices [4, 6]. From this, we show that we have four mode-generating functions instead of one. Note that for each projection of the spin $\sigma = \pm 1$ this function is not necessarily the same for particles and antiparticles. On this basis, we have first considered values of the potential in which the contact interaction separate the interior and exterior regions completely, a situation similar to the one found for the values of the δ-δ' interaction in which we have boundary conditions (10). This kind of configurations have received considerable attention in the context of phenomenological models for quark confinement, such as the MIT bag model [7]. We have studied a massive field using the small mass expansion. For the limiting massless case we have found a one-parameter family of configurations in which the total residue is zero so the energy is defined in an unique way. Furthermore, in the latter positive and negative pressures are found, depending on the values of the free parameter of the potential. Note that only positive pressures, repulsion which tends to expand the sphere, are obtained for the scalar field with the δ-δ' or with MIT boundary conditions, which are recovered as a limiting case [3].

Regarding the Casimir-Lifshitz effect, we have first determined the sign of the interaction energy for two arbitrary magnetodielectrics. If the sign of the $\mathbb{T}$ operator for each body is well defined, this result is independent of the geometry or the matter distribution of the bodies. However, the energy is not by itself a measurable quantity, although as we have shown it determines the behaviour of the interaction force in some cases. This is why we have computed the interaction pressure in cavity configurations. Similarly, we are able to determine the sign of this quantity acting on the surface of a sphere inside a cavity or on a cavity wall. As for the interaction energy, both the matter distribution and the geometry of one of the objects are arbitrary, only assuming a well defined sign of the $\mathbb{T}$ operator. However, we are assuming that the body with the spherical surface and the medium are dielectrics. In consequence, the first obvious generalization is to introduce nontrivial permeability response functions for these materials. In order to do so, we should generalize the results described in [8]. The starting point would be the same, the Lippmann-Schwinger equation in position space, but now considering the whole differential operator. In addition, it can also be explored if the result on the sign of the pressure holds for different geometries. Specifically, if instead of a S^2 sphere we consider a surface $\mathcal{M}$, the mean pressure over $\mathcal{M}$ can be defined in the same way and with the appropriate results of classical electromagnetic scattering on the components of $\mathbb{T}$, the derivation explained in Chapters 6 and 7 would remain unchanged.

References for Conclusions

[1]D. V. Vassilevich, Phys. Rep. **388**, 279 (2003).

[2]M. Bordag, K. Kirsten, and D. Vassilevich, Phys. Rev. D **59**, 085011 (1999).

[3]G. Fucci and C. Romaniega, Manuscript in preparation (2022).

[4]J. Dittrich, P. Exner, and P. Šeba, J. Math. Phys. **30**, 2875 (1989).

[5]P. Kurasov, J. Math. Anal. Appl. **201**, 297 (1996).

[6]M. Bordag, G. L. Klimchitskaya, U. Mohideen, and V. M. Mostepanenko, *Advances in the Casimir Effect* (Oxford University Press, Oxford, 2009).

[7]E. Elizalde, M. Bordag, and K. Kirsten, J. Phys. A Math. Gen. **31**, 1743 (1998).

[8]B. R. Johnson, Appl. Opt. **27**, 4861 (1988).